J|A|C|S
ARTICLES
Published on Web 11/27/2003

Syntheses, Characterizations, and Coordination Chemistry of the 10-Vertex Phosphadicarbaboranes 6-R-*arachno*-6,8,9-$PC_2B_7H_{11}$ and 6-R-*arachno*-6,5,7-$PC_2B_7H_{11}$

Daewon Hong, Scott E. Rathmill, Patrick J. Carroll, and Larry G. Sneddon*

Contribution from the Department of Chemistry, University of Pennsylvania, Philadelphia, Pennsylvania 19104-6323

Received August 7, 2003; E-mail: lsneddon@sas.upenn.edu

Abstract: The 10-vertex phosphadicarbaboranes, 6-R-*arachno*-6,8,9-$PC_2B_7H_{11}$ (**1**) (R = Ph **1a** or Me **1b**) and 6-R-*arachno*-6,5,7-$PC_2B_7H_{11}$ (**2**) (R = Ph **2a** or Me **2b**) have been synthesized using in situ dehydrohalogenation reactions of $RPCl_2$ (R = Ph or Me) with the *arachno*-4,5-$C_2B_7H_{13}$ and *arachno*-4,6-$C_2B_7H_{13}$ carboranes, respectively. X-ray crystallographic determinations in conjunction with DFT/GIAO/NMR calculations and NMR spectroscopic studies have established that both **1** and **2** have open cage structures based on an icosahedron missing two vertexes. The two isomeric compounds differ in the positions of the carbons and bridging hydrogens on the open face. Studies of the reactions of **2a** with BH_3·THF, S_8, and hydrogen peroxide demonstrated that **2a** shows strong donor properties yielding the compounds *endo*-6-H_3B-*exo*-6-Ph-*arachno*-6,5,7-$PC_2B_7H_{11}$ (**3**), *endo*-6-S-*exo*-6-Ph-*arachno*-6,5,7-$PC_2B_7H_{11}$ (**4**), and *endo*-6-O-*exo*-6-Ph-*arachno*-6,5,7-$PC_2B_7H_{11}$ (**5**) in which the BH_3, S, and O substitutents are bonded to an electron lone pair localized at the phosphorus *endo*-position. The reaction of **2a** with an excess of S_8 results in the loss of a framework boron to produce the unique open-cage compound $\mu_{7,8}$-{HS(Ph)P}-*hypho*-7,8-$C_2B_6H_{11}$ (**6**). **2a** also formed the donor complexes *cis*-(η^1-[6-Ph-*arachno*-6,5,7-$PC_2B_7H_{11}$])$_2PtBr_2$ (**7**) and *trans*-(η^1-[6-Ph-*arachno*-6,5,7-$PC_2B_7H_{11}$])$_2PdBr_2$ (**8**) in which the metal fragment is bonded in an η^1-fashion at the phosphorus *endo*-position. In these complexes, **2a** is functioning as a two-electron sigma donor to the metals and can thus be considered as an analogue of the PR_3 ligands in the classical *cis*-$(PPh_3)_2PtBr_2$ and *trans*-$(PPh_3)_2PdBr_2$ coordination complexes. Although **1a** did not show the donor properties exhibited by **2a**, its dianion 6-Ph-6,8,9-$PC_2B_7H_9^{2-}$ (**1a²⁻**) readily formed η^4-coordinated complexes with late transition metals including 8-Ph-7-$(Ph_3P)_2$-*nido*-7,8,10,11-$PtPC_2B_7H_9$ (**9**), 7-Ph-11-(η^5-C_5H_5)-*nido*-11,7,9,10-$CoPC_2B_7H_9$ (**10**), and *commo*-Ni-(7-Ni-8′-Ph-*nido*-8′,10′,11′-$PC_2B_7H_9$)(7-Ni-8-Ph-*nido*-8,10,11-$PC_2B_7H_9$) (**11**).

Introduction

While a variety of phosphacarbaboranes have been prepared and studied,[1] we have only recently reported the syntheses, structures, and chemical reactivities of the first 10-vertex *arachno*-phosphamonocarbaborane 6-R-*arachno*-6,7-PCB_8H_{12} and its conjugate anion 6-R-*arachno*-6,7-$PCB_8H_{11}^-$.[2] These studies showed that, in contrast to the properties observed for the previously known phosphacarbaboranes, the 6-R-*arachno*-6,7-$PCB_8H_{11}^-$ anion exhibited strong donor properties arising from a lone pair of electrons localized on the phosphorus and, accordingly, forms many compounds, including *endo*-6-L-*exo*-6-Ph-*arachno*-6,7-$PCB_8H_{11}^-$ (L = O, S, BH_3), *endo*-6-[CpFe(CO)$_2$]-*exo*-6-Ph-*arachno*-6,7-PCB_8H_{11} and *exo*-6-[$Mn(CO)_5$]-*endo*-6-Ph-*arachno*-6,7-PCB_8H_{11}, in which the 6-R-*arachno*-6,5,7-$PCB_8H_{11}^-$ anion could be considered as an anionic analogue of R_3P.

In this paper, we report the first syntheses and structural characterizations of the 10-vertex phosphadicarbaboranes 6-R-*arachno*-6,8,9-$PC_2B_7H_{11}$ (**1**) and 6-R-*arachno*-6,5,7-$PC_2B_7H_{11}$ (**2**) along with studies that compare the reactivities and coordination properties of these phosphadicarbaboranes with those of the isoelectronic 6-R-*arachno*-6,7-$PCB_8H_{11}^-$ phosphamonocarbaborane anion.[3]

Experimental Section

All manipulations were carried out using standard high-vacuum or inert-atmosphere techniques as described by Shriver.[4]

Materials. Dicholorophenylphosphine, 1,8-bis(dimethylamino)naphthalene (Proton Sponge, PS), sulfur powder, and HCl·Et_2O (1.0 M Et_2O

(1) For reviews of phosphacarbaboranes, see: (a) Stíbr, B. *Collect. Czech. Chem. Commun.* **2002**, *67*, 843−868. (b) Todd, L. J. In *Comprehensive Organometallic Chemistry*; Wilkinson, G., Stone, F. G. A., Abel, E. W., Eds.; Pergamon Press: New York, 1982; Vol. 1, pp 543−553. (c) Todd, L. J. In *Comprehensive Organometallic Chemistry*; Wilkinson, G., Stone, F. G. A., Abel, E. W., Housecroft, C. E., Eds.; Pergamon Press: New York, 1995; Vol. 1, pp 257−273.

(2) (a) Shedlow, A. M.; Kadlecek, D. E.; Clapper, J. C.; Rathmill, S. E.; Carroll, P. J.; Sneddon, L. G. *J. Am. Chem. Soc.* **2003**, *125*, 200−211. (b) Kadlecek, D. E.; Shedlow, A. M.; Kang, S. O.; Carroll, P. J.; Sneddon, L. G. *J. Am. Chem. Soc.* **2003**, *125*, 212−220.

(3) Hong, D.; Rathmill, S. E.; Kadlecek, D. E.; Sneddon, L. G. *Inorg. Chem.* **2000**, *39*, 4996−4997.

(4) Shriver, D. F.; Drezdzon, M. A. *Manipulation of Air-Sensitive Compounds*, 2nd ed.; Wiley: New York, 1986.

10.1021/ja037799+ CCC: $25.00

solution) were purchased from Aldrich and used as received. Dichloromethylphosphine, $CpCo(CO)_2$, $(Ph_3P)_2PtCl_2$, $PtBr_2$, and $PdBr_2$ were purchased from Strem and used as received. Oil dispersed NaH was purchased from Aldrich, washed with dry hexanes under an N_2 atmosphere, and dried under high vacuum prior to use. The 1,2-dimethoxyethane (DME), toluene, and dichloromethane were dried by passing through an activated alumina column prior to use. HPLC grade hexanes and chloroform were purchased from Fisher and used as received. The *arachno*-4,5-$C_2B_7H_{13}$[5] and *arachno*-4,6-$C_2B_7H_{13}$[6] were prepared according to literature procedures.

Physical Measurements. NMR data are presented in Table 1. ^{1}H NMR spectra at 500.4 MHz, ^{11}B NMR spectra at 160.5 MHz, and ^{13}C NMR at 125.8 MHz were obtained on a Bruker AM-500 spectrometer equipped with the appropriate decoupling accessories. ^{31}P NMR spectra at 145.8 MHz were obtained on a Bruker AM-360 spectrometer. All ^{11}B chemical shifts are referenced to external $BF_3{\cdot}Et_2O$ (0.00 ppm), with a negative sign indicating an upfield shift. All ^{1}H and ^{13}C chemical shifts were measured relative to internal residual protons or carbons in the lock solvents and are referenced to Me_4Si (0.00 ppm). All ^{31}P chemical shifts are referenced to external 85% H_3PO_4 (0.0 ppm) with a negative sign indicating an upfield shift. Infrared spectra were obtained on a Perkin-Elmer 1430 spectrophotometer. Elemental analyses were performed at the University of Pennsylvania microanalysis facility. Mass spectra were recorded on a Micromass Autospec spectrometer. Melting points were obtained on a standard melting point apparatus and are uncorrected.

6-Ph-*arachno*-6,8,9-$PC_2B_7H_{11}$ (1a). A 0.36 g (3.2 mmol) sample of *arachno*-4,5-$C_2B_7H_{13}$ was dissolved in 20 mL of DME under an Ar atmosphere. A 2.05 g (9.6 mmol, 3 equiv) sample of Proton Sponge was then added while the solution was maintained at 0 °C. The mixture was stirred for ∼1 h at room temperature. A 0.43 mL (3.2 mmol, 1 equiv) sample of $PhPCl_2$ was then added via syringe at 0 °C, and the contents were allowed to warm to room temperature. A ^{11}B NMR spectrum taken at this point was consistent with the formation of the 6-Ph-*arachno*-6,5,10-$PC_2B_7H_{10}^-$ anion (vide infra). Acidification with excess $HCl{\cdot}Et_2O$ (1.0 M, 12 mL) at −78 °C then generated 6-Ph-*arachno*-6,8,9-$PC_2B_7H_{11}$ (**1a**). The solution was filtered to remove the precipitate in an Ar-filled glovebag. The filtrate was removed to the vacuum line, and the volatiles were evaporated in vacuo. The product was extracted with 30 mL of toluene from the residual materials. After toluene removal, 0.48 g (2.2 mmol, 68%) of solid **1a** was obtained. If necessary, the product was purified by flash silica gel chromatography using hexanes/dichloromethane (4:1, v/v) as the eluent. For **1a**: mp 93 °C. Anal. Calcd: C, 43.90; H, 7.37. Found: C, 44.37; H, 7.07. HRMS (CI neg) (*m*/*e*) calcd for $^{12}C_8{}^1H_{16}{}^{11}B_7{}^{31}P$ 220.1650, found 220.1654; IR (NaCl, cm^{-1}) 3040 (m), 2940 (s), 2910 (s), 2860 (m), 2540 (s), 2390 (w), 2310 (w), 1730 (m), 1570 (w), 1460 (m), 1420 (s), 1350 (m), 1260 (m), 1050 (m), 950 (m), 740 (m), 680 (m).

6-Me-*arachno*-6,8,9-$PC_2B_7H_{11}$ (1b). A 0.39 g (3.5 mmol) sample of *arachno*-4,5-$C_2B_7H_{13}$ was dissolved in 15 mL of DME under an Ar atmosphere. Then, 2.22 g (10.4 mmol, 3 equiv) of Proton Sponge was added at 0 °C. The mixture was stirred for ∼30 min at room temperature. A 0.31 mL (3.5 mmol, 1 equiv) sample of $MePCl_2$ was then added via syringe at 0 °C, and the contents were allowed to warm to room temperature. After 13 h, excess $HCl{\cdot}Et_2O$ (1.0 M, 12 mL) was added at −78 °C. The solution was then filtered to remove the precipitate in an Ar-filled glovebag. The filtrate was removed to the vacuum line, and the volatiles were evaporated in vacuo. The product was extracted with 30 mL of toluene from the residual materials. After toluene removal, 0.27 g (1.7 mmol, 49%) of oily **1b** was obtained. If necessary, the product was re-extracted with toluene or hexanes. For **1b**: HRMS (CI neg) (*m*/*e*) calcd for $^{12}C_3{}^1H_{14}{}^{11}B_7{}^{31}P$ 158.1485, found 158.1481; IR (CH_2Cl_2, NaCl, cm^{-1}) 2900 (w), 2650 (s), 2610 (s), 2550 (s), 2420 (s), 2350 (m), 1470 (m), 1400 (s), 1270 (m), 1100 (m), 1050 (m), 1020 (m), 980 (s), 960 (m), 920 (w), 900 (s), 880 (m).

6-Ph-*arachno*-6,5,7-$PC_2B_7H_{11}$ (2a). A 0.161 g (1.4 mmol) sample of *arachno*-4,6-$C_2B_7H_{13}$ was dissolved in 20 mL of DME under an N_2 atmosphere. Then, 0.614 g (2.9 mmol) of Proton Sponge was added to the solution at 0 °C. Stirring was continued for 1 h at room temperature, and then 0.19 mL of $PhPCl_2$ was added dropwise via syringe at 0 °C. Immediately, a white precipitate formed. The mixture was brought to room temperature and stirred for 2 h. The reaction mixture was filtered in the glovebag, resulting in a pale yellow solution. The filtrate was removed to a 250 mL one-piece glass vessel with a sidearm, and the solvent was then carefully removed in vacuo, to give a mixture of white and yellow materials visibly separated inside of the glass vessel. The yellow material was carefully removed using dichloromethane, which gave white solid **2a** (0.140 g, 0.64 mmol, 46%). If necessary, the product was re-extracted with toluene or hexanes. For **2a**: mp 74 °C. Anal. Calcd for $C_8H_{16}B_7P{\cdot}{}^1/_8CH_2Cl_2$: C, 42.53; H, 7.14. Found: C, 42.51; H, 7.53. HRMS (CI neg) (*m*/*e*) calcd for $^{12}C_8{}^1H_{16}{}^{11}B_7{}^{31}P$ 220.1641, found 220.1640; IR (CH_2Cl_2, NaCl, cm^{-1}) 3150 (w, br), 2500 (s), 1450 (w), 1150 (s), 1020 (s).

6-Me-*arachno*-6,5,7-$PC_2B_7H_{11}$ (2b). A 0.45 g (4.0 mmol) sample of *arachno*-4,6-$C_2B_7H_{13}$ was dissolved in 40 mL of THF under an N_2 atmosphere. Then, 1.83 g (8.5 mmol) of Proton Sponge was added to this solution. After the solution was stirred for 1 h at room temperature, 0.40 mL of $MePCl_2$ was added dropwise via syringe at 0 °C. Immediately, a white precipitate formed. The mixture was brought to room temperature and stirred for 1 h. The crude product was then vacuum distilled at 90 °C for 3 h, to give 0.31 g (2.0 mmol, 50%) of a pale yellow oily **2b**. For **2b**: Anal. Calcd: C, 22.77; H, 8.86. Found: C, 23.44; H, 9.46. LRMS (*m*/*e*) calcd for $^{12}C_3{}^1H_{14}{}^{11}B_7{}^{31}P$ 158, found 158 (seven-boron isotope pattern); IR (NaCl, neat, cm^{-1}) 3050 (m), 2560 (s), 2050 (w), 1500 (w), 1425 (m), 1390 (m), 1280 (m), 1200 (w), 1140 (w), 1050 (s), 970 (m), 920 (s), 880 (m), 850 (s), 810 (m), 780 (m).

Reaction of 6-Ph-*arachno*-6,8,9-$PC_2B_7H_{11}$ (1a) and BH_3. A 0.5 mL sample of a THF-d_8 solution containing 56 mg (0.3 mmol) of **1a** was mixed with an excess amount of $BH_3{\cdot}THF$ (0.5 mL, 1.0 M THF) at room temperature. No reaction was observed by NMR spectroscopy.

Reaction of 6-Ph-*arachno*-6,5,7-$PC_2B_7H_{11}$ (2a) and BH_3. A **2a** THF solution (**A**) was prepared by dissolving 0.174 g (0.79 mmol) of **2a** in 3.00 mL of freshly distilled THF. A fresh $BH_3{\cdot}THF$ (1.0 M THF) solution (**B**) was mixed with **A** in ratios of 0.3/0.1 (**S1**), 0.2/0.2 (**S2**), 0.2/0.3 (**S3**), and 0.1/0.3 (**S4**) (**A**/**B**, mL/mL) under an inert atmosphere at room temperature. Immediately, *endo*-6-H_3B-*exo*-6-Ph-*arachno*-6,5,7-$PC_2B_7H_{11}$ (**3**) was formed. In each case, the amounts of **3** (M) and free **2a** (M) were calculated by peak integrations of the −21.6 ppm (for **3**) and the −33.0 ppm (for **2a**) peaks in the ^{11}B NMR spectra. These results are summarized in Table 2.

Reaction of 6-Ph-*arachno*-6,8,9-$PC_2B_7H_{11}$ (1a) and Sulfur. A 0.5 mL aliquot of $CHCl_3$ solution containing ∼5 mg (∼0.02 mmol) of **1a** was mixed with ∼5 mg (∼0.2 mmol) of S_8 at room temperature. No reaction was observed in 3 h by ^{11}B NMR spectroscopy.

Reaction of 6-Ph-*arachno*-6,5,7-$PC_2B_7H_{11}$ (2a) and Sulfur: Formation of *endo*-6-S-*exo*-6-Ph-*arachno*-6,5,7-$PC_2B_7H_{11}$ (4). A 0.219 g (1.0 mmol) sample of **2a** was reacted with 0.048 g (1.5 mmol) of sulfur powder in 17 mL of DME at room temperature. The solution was stirred at room temperature for 22 h. After the mixture was filtered, the volatiles were removed in vacuo to give 0.25 g (>90% yield) of **4**. For **4**: HRMS (*m*/*e*) calcd for $^{12}C_8{}^1H_{16}{}^{11}B_7{}^{31}P^{32}S$ 252.1362, found 252.1348; IR (CH_2Cl_2, NaCl, cm^{-1}) 3150 (m, br), 2500 (s), 1950 (w, br), 1450 (w), 1440 (m, br), 1250 (m, br), 1090 (m, br), 910 (m).

Reaction of 6-Ph-*arachno*-6,8,9-$PC_2B_7H_{11}$ (1a) and Peroxide. A 0.5 mL sample of a THF-d_8 solution containing ∼5 mg (∼0.02 mmol)

(5) (a) Hermánek, S.; Jelínek, T.; Plesek, J.; Stíbr, B.; Fusek, J. *J. Chem. Soc., Chem. Commun.* **1987**, 927−928. (b) Stíbr, B.; Plesek, J.; Hermánek, S. *Inorg. Synth.* **1983**, *22*, 237−239.

(6) Garrett, P. M.; George, T. A.; Hawthorne, M. F. *Inorg. Chem.* **1969**, *8*, 2008−2009.

Table 1. NMR Data[a]

compounds	nucleus	δ (multiplicity, assignment, J (Hz))
6-Ph-*arachno*-6,8,9-$PC_2B_7H_{11}$ (**1a**)[b]	^{11}B	−5.5 (d, B2,4; J_{BH} 163), −12.0 (d, B5; J_{BH} 163, J_{BHB} 24), −13.6 (d, B7; J_{BH} 147), −19.7 (d, B10; J_{BH} 153, J_{BHB} 43), −28.5 (d, B1; J_{BH} 154), −48.4 (d, B3; J_{BH} 159)
	^{1}H{^{11}B}	7.47, 7.16, 6.93 (m, 5, phenyl), 3.26 (1, BH), 3.13 (1, BH), 2.73 (1, BH), 2.39 (1, BH), 2.25 (2, BH), 1.47 (1, cage-CH), 1.08 (1, BH), 0.46 (1, cage-CH), −0.72 (1, cage-CH), −2.01 (1, BHB)
	^{13}C	131.5 (J_{CP} 13), 128.6, 128.0, 24.4 (C8, J_{CB} 47), 13.2 (C9; t of d, J_{CP} 49, $J_{CHendo}\sim$160, $J_{CHexo}\sim$160)
	^{31}P	−163.5 (P6)
Ia[c]	^{11}B (calc)	−4.2 (B4), −4.6 (B2), −10.8 (B5), −14.6 (B7), −22.3 (B10), −30.5 (B1), −49.5 (B3)
	^{13}C(calc)	132.3−142.6 (phenyl), 30.5 (C8), 14.3 (C9)
	^{31}P(calc)	−140.1 (P6)
6-Ph-*arachno*-6,8,9-$PC_2B_7H_{10}^-$ (**1a**$^-$)[d]	^{11}B	−2.7 (d, B2; $J_{BH}\sim$183), −4.1 (d, B4; $J_{BH}\sim$155), −17.3 (d, B5,7; J_{BH} 141), −18.8 (d, B10; $J_{BH}\sim$136), −41.5 (d, B1,3; J_{BH} 138)
Ia$^-$[c]	^{11}B (calc)	−0.7 (B2), −4.9 (B4), −10.1 (B5), −14.5 (B7), −20.2 (B10), −42.2 (B3), −43.5 (B1)
Ib$^-$[c]	^{11}B (calc)	0.1 (B2), −1.3 (B4), −16.3 (B7), −16.7 (B5), −19.4 (B10), −42.3 (B1), −42.8 (B1)
6-Ph-*arachno*-6,8,9-$PC_2B_7H_9^{2-}$ (**1a**$^{2-}$)	^{11}B	1.2 (1), −18.3 (1), −41.3 (1), −42.9 (2), −44.2 (2)
Ib^{2-}[c]	^{11}B (calc)	6.1 (B4), −14.1 (B10), −38.7 (B1), −41.1 (B3), −42.6 (B7), −50.3 (B2), −51.2 (B5)
6-Me-*arachno*-6,8,9-$PC_2B_7H_{11}$ (**1b**)[b]	^{11}B	−6.0 (d, B2;J_{BH} 157), −6.7 (d, B4; J_{BH} > 120, overlapped), −11.1 (d, B5; J_{BH} 169), −12.2 (d, B7; J_{BH} 148), −19.9 (d, B10; J_{BH} 146), −28.7 (d, B1; J_{BH} 167), −48.8 (d, B3; J_{BH} 150)
	^{1}H{^{11}B}	2.95 (1, BH), 2.79 (1, BH), 2.66 (1, BH), 2.20 (2, BH), 2.09 (1, BH), 1.39 (1, cage-CH), 1.03 (1, BH), 0.75 (3, CH_3), 0.38 (1, cage-CH), −0.90 (1, cage-CH), −2.15 (1, BHB)
	^{13}C{^{1}H}	25.5 (C8, J_{CB} 63), 12.8 (C9, J_{CP} 43), 7.3 (*C*H$_3$, J_{CP} 19)
	^{31}P	−184.3 (P6)
Ib[c]	^{11}B (calc)	−4.8 (B2), −6.6 (B4), −10.7 (B5), −11.0 (B7), −22.1 (B10), −30.3 (B1), −50.3 (B3)
	^{13}C(calc)	31.5 (C8), 14.4 (C9), 11.4 (C11)
	^{31}P(calc)	−169.5 (P6)
6-Ph-*arachno*-6,5,7-$PC_2B_7H_{11}$ (**2a**)	^{11}B[b]	−1.6 (d, B4; J_{BH} 178), −7.4 (d, B8,10; J_{BH} 149), −33.0 (d, B1,3,9; J_{BH} 167), −41.6 (d, B2; J_{BH} 149)
	^{1}H{^{11}B}[b]	7.35−6.76 (5, phenyl), 2.95 (3, BH), 2.06 (2, BH), 1.97 (1, BH), 0.82 (s, 2H, cage-CH), 0.80 (1, BH), −2.98 (2, BHB)
	^{13}C{^{1}H}[e,f]	130.2−127.9 (phenyl), 3.2 (C5,7J_{CP} 55)
	^{31}P[b]	−72.5 (P6)
Va[c]	^{11}B (calc)	−2.3 (B4), −8.9 (B8,10), −33.6 (B5,7), −36.7 (B9), −45.7 (B2)
	^{13}C (calc)	146.9−132.8 (phenyl), 5.3 (C5,7)
	^{31}P (calc)	−49.9 (P6)
6-Me-*arachno*-6,5,7-$PC_2B_7H_{11}$ (**2b**)	^{11}B[b]	−1.9 (d, B4;J_{BH} 176), −6.9 (d, B8,10; J_{BH} 149), −33.5 (d, B1,3,9; J_{BH} 167), −41.9 (d, B2; J_{BH} 148)
	^{1}H{^{11}B}[f]	3.09 (1, BH), 2.56 (2, BH), 1.59 (2, BH), 1.56 (d, 3, CH_3; J_{PH} 11), 1.37 (1, BH), 1.06 (2, cage-CH), 0.07 (1, BH), −3.23 (2, BHB)
	^{13}C{^{1}H}[e,f]	18.1 (*C*H$_3$; J_{CP} 43), 2.4 (C5,7, J_{CP} 52)
	^{31}P[b]	−65.2 (P6)
Vb[c]	^{11}B (calc)	−3.8 (B4), −8.9 (B8,10), −34.6 (B1,3), −36.5 (B9), −46.0 (B2)
	^{13}C(calc)	22.8 (C11), 8.0 (C5,7)
	^{31}P(calc)	−55.0 (P6)
6-Ph-*arachno*-6,5,10-$PC_2B_7H_{10}^-$	^{11}B{^{1}H}[g]	9.7, 1.6, −16.6, −23.7, −28.6, −41.6, −43.9
II$^-$	^{11}B (calc)	11.4 (B8), 0.0 (B4), −15.0 (B2), −20.4 (B7), −34.4 (B9), −36.7 (B3), −46.8 (B1)
endo-6-BH_3-*exo*-6-Ph-*arachno*-6,5,7-$PC_2B_7H_{11}$(**3**)[d,g]	^{11}B	4.4 (B4), −6.3 (B8,10), −21.6 (B1,3,4), −39.9 (BH_3), −43.7 (B2)
VI[c]	^{11}B (calc)	2.5 (B4), −8.7 (B10), −8.9 (B8), −22.3 (B3), −23.0 (B1), −24.9 (B9), −44.0 (BH_3), −47.1 (B2)
endo-6-S-*exo*-6-Ph-*arachno*-6,5,7-$PC_2B_7H_{11}$ (**4**)[b]	^{11}B	0.3 (d, B4; J_{BH} 178), −7.4 (d, B8,10; J_{BH} 150), −14.3 (d, B1,3; J_{BH} 163), −16.5 (d, B9; J_{BH} 151), −44.9 (d, B2; J_{BH} 150)
	^{13}C{^{1}H}	127.9−133.1 (phenyl), 15.0 (C7,8)
	^{31}P	5.6 (P6)
VII[c]	^{11}B (calc)	0.0 (B4), −8.1 (B8,10), −13.0 (B1,3), −18.5 (B9), −46.7 (B2)
	^{13}C(calc)	131.5−150.2 (phenyl), 21.8 (C7,8)
	^{31}P(calc)	22.4 (P6)
endo-6-O-*exo*-6-Ph-*arachno*-6,5,7-$PC_2B_7H_{11}$ (**5**)[b]	^{11}B	−0.6 (d, B4; J_{BH} 175), −4.7 (d, B8,10; J_{BH} 144), −12.0 (d, B1,3; J_{BH} 163), −19.5 (d, B9; J_{BH} 154), −46.1 (d, B2; J_{BH} 146)
	^{31}P	−18.7 (P6)
VIII[c]	^{11}B (calc)	−2.1 (B4), −7.1 (B8,10), −12.3 (B1,3), −21.6 (B9), −49.2 (B2)
	^{31}P(calc)	−18.9 (P6)
$\mu_{7,8}$-{HS(Ph)P}-*hypho*-7,8-$C_2B_6H_{11}$ (**6**)[b]	^{11}B	−7.8 (d, B4,6, J_{BH} 135), −25.3 (d, B5, J_{BH} 144), −28.4 (d, J_{BH}, B2,3, 132), −54.0 (d, J_{BH}, B1, 141)
	^{1}H{^{11}B}	8.09−7.59 (phenyl), 2.37 (2, BH), 2.30 (1, BH), 1.79 (2, BH), 1.55 (SH), 1.30 (2, cage-CH), −1.05 (1, BH), −1.49 (d, B*H*B, $^3J_{PH}$ 35), −1.83 (2, B*H*B)
	^{13}C{^{1}H}	133.8−129.2 (phenyl), 2.4 (C7,8)
	^{31}P	94.4 (P9)
IX[c]	^{11}B(calc)	−9.3 (B4,6), −29.1 (B5), −30.1 (B2,3), −58.9 (B1)
	^{13}C(calc)	137.9−133.3 (phenyl), 13.7 (C7,8)
	^{31}P(calc)	94.0 (P9)

Table 1 (Continued)

compounds	nucleus	δ (multiplicity, assignment, J (Hz))
cis-(η^1-[6-Ph-*arachno*-6,5,7-$PC_2B_7H_{11}$])$_2$-$PtBr_2$ (**7**)[f]	^{11}B	9.8 (d, J_{BH} 139), 2.4 (d, J_{BH} 150), −4.7 (br), −20.2 (br), −22.3 (br), −34.2 (br), −42.5 (d, J_{BH} 151)
	^{1}H{^{11}B}	7.96−7.29 (m, phenyl), 3.39 (BH), 2.99 (BH), 2.75 (BH), 2.49 (BH), 2.14 (BH), 1.56 (BH), 1.43 (cage-CH), 1.31 (BH), 0.93 (cage-CH), −1.45 (BHB), −1.93 (BHB)
	^{13}C{^{1}H}	132.0−128.9 (phenyl), 4.6 (cage C)
	^{31}P	−5.2 (J_{Pt-P} 3010); (−8.2, J_{Pt-P} 3010)[h]
trans-(η^1-[6-Ph-*arachno*-6,5,7-$PC_2B_7H_{11}$])$_2$$PdBr_2$ (**8**)[f]	^{11}B	1.7 (d, J_{BH} 140), −4.1 (br), −20.7 (br), −23.8 (br) −23.0 (br), −41.9 (d, J_{BH} 148)
8-Ph-7-(Ph_3P)$_2$-*nido*-7,8,10,11-$PtPC_2B_7H_9$ (**9**)[f]	^{11}B	−6.1 (d, J_{BH} ∼100), −12.6 (d, J_{BH} ∼109), −15.6 (d, J_{BH} 143), −17.7 (br), −21.8 (br), −37.2 (d, J_{BH} 140)
	^{1}H{^{11}B}	7.59−6.98 (phenyl), 3.94 (1, BH), 3.10 (1, CH), 2.47 (1, BH), 2.17 (1, BH), 1.81 (1, BH), 1.67 (1, CH), 1.54 (1, BH), 0.71 (1, BH)
	^{13}C{^{1}H}	134.4−127.7 (phenyl), 54.2 (cage C), 43.6 (cage C)
	^{31}P	23.0 (J_{Pt-P} 3596), 14.8 (J_{Pt-P} 4218, J_{PP} 18), 14.3 (J_{Pt-P} 4236, J_{PP} 17)
7-Ph-11-(η^5-C_5H_5)-*nido*-11,7,9,10-$CoPC_2B_7H_9$ (**10**)[f]	^{11}B	−3.4 (d, J_{BH} 152), −7.1 (d, J_{BH} 149), −9.0 (d, J_{BH} 152), −15.4 (d, J_{BH} 151, J_{BP} 61), −17.2 (d, J_{BH} 151), −19.2 (d, J_{BH} 169), −35.6 (J_{BH} 148)
	^{1}H{^{11}B}	7.64−7.42 (5, phenyl), 5.16 (5, C_5H_5), 3.68 (1, CH), 3.34 (1, BH), 3.07 (1, BH), 2.79 (1, BH), 2.40 (2, CH, BH), 1.73 (2, BH), 1.14 (1, BH)
	^{13}C{^{1}H}	133.5−129.3 (phenyl), 86.7 (C_5H_5), 59.2, 47.8 (J_{CP} 34)
	^{31}P	−31.5
commo-Ni-(7-Ni-8′-Ph-8′,10′,11′-*nido*-$PC_2B_7H_9$)-(7-Ni-8-Ph-8,10,11-*nido*-$PC_2B_7H_9$) (**11**)[f]	^{11}B	−3.3 (d, J_{BH} 158), −5.5 (d, J_{BH} 146), −12.1 (d, J_{BH} 142), −19.4 (d, J_{BH} ∼126, overlapped), −20.2 (d, J_{BH} ∼158, overlapped), −30.6 (d, J_{BH} 150)
	^{31}P	−33.1

[a] ^{1}H NMR (500.4 MHz), ^{11}B NMR (160.5 MHz), ^{13}C NMR (125.8 MHz), ^{31}P NMR (145.8 MHz). [b] C_6D_6. [c] DFT/GIAO (B3LYP/6-311G*). [d] THF-d_8. [e] Measured at −83 °C. [f] CD_2Cl_2. [g] ^{11}B NMR (64.2 MHz). [h] See text.

Table 2. Summary of ^{11}B NMR Integration Data for the Reaction of **2a** with BH_3·THF

	S1	S2	S3	S4
[**3**] (−21.6 ppm)	0.096	0.082	0.071	0.045
[**2a**] (−33.0 ppm)	0.100	0.050	0.035	0.021
K_{eq}[a]	6.1	3.9	3.8	3.0
ΔG (kcal/mol)	−4.5	−3.4	−3.3	−2.7

[a] $K_{eq} = [\mathbf{3}]_{eq}/[\mathbf{2a}]_{eq}[BH_3{\cdot}THF]_{eq}$.

of **1a** was mixed with ∼0.05 mL of H_2O_2 at room temperature. Decomposition of **1a** to borate was observed by NMR spectroscopy.

Reaction of 6-Ph-*arachno*-6,5,7-$PC_2B_7H_{11}$ (2a) and Peroxide: Formation of *endo*-6-O-*exo*-6-Ph-*arachno*-6,5,7-$PC_2B_7H_{11}$ (5). A sample (∼10 mg, ∼0.05 mmol) of **2a** was dissolved in 0.5 mL of THF-d_8 containing a small amount of peroxide at room temperature. Immediately, gas was generated, and ^{11}B and ^{31}P NMR analyses indicated the formation of *endo*-6-O-*exo*-6-Ph-*arachno*-6,5,7-$PC_2B_7H_{11}$ (**5**). **5** proved to be too unstable to be isolated in a pure form. For **5**: HRMS (CI neg) (*m*/*e*) calcd for $^{12}C_8{}^1H_{16}{}^{11}B_7{}^{31}P^{16}O$, 236.1590, found 236.1600.

Reaction of 6-Ph-*arachno*-6,5,7-$PC_2B_7H_{11}$ (2a) with Excess Sulfur: Synthesis of $\mu_{7,8}$-{HS(Ph)P}-*hypho*-7,8-$C_2B_6H_{11}$ (6). A 0.28 g (1.3 mmol) sample of **2a** was reacted with 0.3 g (9.4 mmol, excess) of sulfur powder in 10 mL of DME at room temperature. The solution was stirred at room temperature for 8 h. After the mixture was filtered, the volatiles were removed in vacuo. The residue was purified by preparatory TLC (hexanes/CH_2Cl_2 = 1:1, v/v) to give 0.16 g (0.67 mmol, 52%) of yellow liquid **6**. For **6**: HRMS (CI neg) (*m*/*e*) calcd for $^{12}C_8{}^1H_{17}{}^{11}B_6{}^{31}P^{32}S$ 242.1347, found 242.1348; IR (CH_2Cl_2 sol, NaCl, cm^{-1}) 3150 (m), 2910 (m), 2540 (s), 1980 (w), 1850 (w), 1590 (w), 1480 (m), 1430 (s), 1310 (m), 1170 (m), 1100 (s), 1050 (s), 960 (m), 910 (s).

***cis*-(η^1-[6-Ph-*arachno*-6,5,7-$PC_2B_7H_{11}$])$_2$$PtBr_2$ (7).** A 0.16 g (0.73 mmol) sample of **2a** was dissolved in 5 mL of DME at room temperature. Then 0.114 g (0.32 mmol) of $PtBr_2$ was added. The reaction mixture was stirred at room temperature for 2.5 h. After the mixture was filtered, the solvent was removed in vacuo. A 0.079 g (0.10 mmol, 31%) sample of yellow **7** was obtained after preparative TLC (pentane/CH_2Cl_2 = 2:1, v/v). For **7**: mp 198−200 °C. Anal. Calcd: C, 24.25; H, 4.07. Found: C, 23.30; H, 4.16. IR (CH_2Cl_2 sol, NaCl, cm^{-1}) 3150 (w), 2550 (s), 1480 (s), 1320 (s), 1150 (s), 1050 (s), 950 (m), 870 (s).

***trans*-(η^1-[6-Ph-*arachno*-6,5,7-$PC_2B_7H_{11}$])$_2$$PdBr_2$ (8).** A 0.40 g (1.45 mmol) sample of **2a** was dissolved in 15 mL of DME at room temperature. Then, 0.116 g (0.62 mmol) of $PdBr_2$ was added. The reaction mixture was stirred at room temperature for 21 h. Workup of the reaction as described above yielded a mixture containing, according to the ^{31}P and ^{1}H NMR spectra, at least two products that were inseparable by silica gel column chromatography. Crystals of **8** (>10 mg) *trans*-(η^1-[6-Ph-*arachno*-6,5,7-$PC_2B_7H_{11}$])$_2$$PdBr_2$ were obtained by crystallization from this mixture, but it was not possible to isolate other products in sufficient quantities for characterization. For **8**: Anal. Calcd for $C_{16}H_{32}B_{14}Br_2P_2Pd{\cdot}{}^1/_6C_6H_{14}$: C, 28.4; H, 4.81. Found: C, 28.4; H, 5.03.

8-Ph-7-(Ph_3P)$_2$-*nido*-7,8,10,11-$PtPC_2B_7H_9$ (9). A 0.26 g (1.2 mmol) sample of **1a** was dissolved in 10 mL of DME under an inert atmosphere. A 1.8 mL aliquot of MeLi (1.4 M Et_2O solution) was added dropwise at −78 °C. After 6-Ph-6,8,9-$PC_2B_7H_9^{2-}$ (**1a**$^{2-}$) formation was observed by ^{11}B NMR spectroscopy, 0.95 g (1.2 mmol) of (Ph_3P)$_2$-$PtCl_2$ was added to this reaction mixture at −78 °C. The mixture was stirred at room temperature for 18 h. After the mixture was filtered, the volatiles were removed in vacuo. The resulting dark brown species was chromatographed on preparative TLC plates (hexanes/CH_2Cl_2 = 3:2, v/v) to give 0.38 g (0.41 mmol, 34%) of yellow **9**. For **9**: mp 148−150 °C. Anal. Calcd: C, 56.43; H, 4.74. Found: C, 55.60; H, 4.66. IR (CH_2Cl_2 sol, NaCl, cm^{-1}) 2890 (s), 2800 (m), 2530 (s), 1460 (s), 1420 (s), 1180 (m), 1110 (m), 1090 (m), 680 (s).

7-Ph-11-(η^5-C_5H_5)-*nido*-11,7,9,10-$CoPC_2B_7H_9$ (10). A 0.48 g (2.2 mmol) sample of **1a** was dissolved in 20 mL of DME at room temperature under an inert atmosphere. A 0.44 g (2.4 mmol) sample of $CpCo(CO)_2$ was then added dropwise to this solution at room temperature. The reaction mixture was next heated at 70 °C under an inert atmosphere for 66 h. After the solution was filtered, the solvent was vacuum evaporated yielding a deep brown crude product (0.69 g, 2.0 mmol). After this crude product was purified by preparative TLC (hexanes/CH_2Cl_2 = 4:1, v/v), 0.11 g (0.33 mmol, 15%) of dark red **10**

was obtained. For **10**: mp 190−192 °C. Anal. Calcd: C, 45.81; H, 5.62. Found: C, 45.10; H, 5.72. HRMS (CI neg) (*m*/*e*) calcd for $^{12}C_{13}{}^{1}H_{19}{}^{11}B_{7}{}^{31}P^{59}Co$ 342.1208, found 342.1224. IR (CH_2Cl_2 sol, NaCl, cm^{-1}) 3080 (w), 2550 (s), 1460 (m), 1420 (m), 1400 (m), 1090 (s), 1050 (m), 1000 (s), 810 (s).

***commo*-Ni-(7-Ni-8′-Ph-*nido*-8′,10′,11′-$PC_2B_7H_9$)(7-Ni-8-Ph-*nido*-8,10,11-$PC_2B_7H_9$) (11).** A 0.295 g (1.35 mmol) sample of **1a** was dissolved in 15 mL of DME under an inert atmosphere. A 1.0 mL aliquot of MeLi (1.4 M Et_2O solution) was introduced dropwise at −78 °C. To this mixture, 0.148 g (0.68 mmol) of $NiBr_2$ was added, resulting in an immediate color change. The reaction mixture was stirred at room temperature for 24 h. After the precipitate was filtered off, the solvent was removed in vacuo. After preparative TLC (hexanes/CH_2Cl_2 = 4:1, v/v), 0.034 g (R_f = 0.45, 0.069 mmol, 10%) of **11** were obtained as a yellow solid. For **11**, Anal. Calcd: C, 39.03; H, 5.73. Found: C, 39.23; H, 5.61. HRMS (*m*/*e*) calcd for $^{12}C_{16}{}^{1}H_{28}{}^{11}B_{14}{}^{31}P_2Ni$ 494.2322, found 494.2308. An additional product (TLC, R_f = 0.4) of the reaction, which according to its mass spectrum is an isomer of **11**, could not be isolated sufficiently pure for complete characterization.

Collection and Reduction of the Data. X-ray intensity data for **1a** (Penn 3176), **2a** (Penn 3184), **7** (Penn 3183), **8** (Penn 3198), **9** (Penn 3182), **10** (Penn 3171), and **11** (Penn 3180) were collected on either a Rigaku R-AXIS IIc or Mercury CCD (for **8**) area detector employing graphite-monochromated Mo Kα radiation (λ = 0.71069 Å). Indexing was performed from a series of 1° oscillation images, and a crystal-to-detector distance of 82 mm was employed, except for **8** where a series of four 0.5° oscillation images and a 35 mm distance were used. Oscillation images were processed to produce a listing of unaveraged F^2 and $\sigma(F^2)$ values which were then passed to the teXsan[7] program package for further processing and structure solution on Silicon Graphics Indigo R4000 or O2 computers. The intensity data were corrected for Lorentz and polarization effects. Absorption correction data for **8** and **9** were made using REQAB[8] (minimum and maximum transmission 0.599, 1.000 for **8**; 0.748, 1.000 for **9**). **8** was found to be twinned by a rotation of 180° about the normal to 001, and twin indexing and processing of twinned data were performed by the TwinSolve[9] module of CrystalClear.

Solution and Refinement of the Structure. The structures were solved by direct methods (SIR92)[10] except for **9** which was solved by the Patterson method (DIRDIF).[11] Refinements were by full-matrix least squares based on F^2 using SHELXL-93.[12] All reflections were used during refinement (F^2's that were experimentally negative were replaced by F^2 = 0). Crystal and refinement data are given in Table 3. Refined positional parameters, refined thermal parameters, bond distances, and angles are given in the Supporting Information. Non-hydrogen atoms were refined anisotropically. All cage hydrogen atoms were refined isotropically. All hydrogen atoms of **1a** and **11** were refined isotropically. Cage hydrogen atoms of **7** and all the hydrogen atoms of **8** were included as constant contribution to the structure and were not refined. All other hydrogen atoms were refined using a "riding" model. In **10**, the cyclopentadienyl ligand is rotationally disordered through two approximately equally populated orientations. The multiplicities of the two orientations refined to 0.49(3) and 0.51(3).

Computational Studies. The DFT/GIAO/NMR method,[13] using either the Gaussian 94[14] or 98[15] program, was used in a manner similar to that previously described.[2,16,17] The geometries were fully optimized at the B3LYP/6-311G* level within the specified symmetry constraints (using the standard basis sets included) on a (4)-processor Origin 200 computer running IRIX 6.5.6. A vibrational frequency analysis was carried out on each optimized geometry at the B3LYP/6-311G* level with a true minimum found for each structure (i.e., possessing no imaginary frequencies). The NMR chemical shifts were calculated at the B3LYP/6-311G* level using the GIAO option within Gaussian 94/98. The ^{11}B NMR GIAO chemical shifts are referenced to $BF_3{\cdot}Et_2O$ using an absolute shielding constant of 102.24.[17] The ^{13}C NMR GIAO chemical shifts are referenced to TMS using an absolute shielding constant of 184.38 and are corrected as described previously.[16,17] The ^{31}P NMR GIAO chemical shifts were first referenced to PH_3 using an absolute shielding constant of 557.2396 ppm and then converted to the H_3PO_4 reference scale using the experimental value of $\delta(PH_3)$ = −240 ppm.[16b]

Results and Discussion

Syntheses and Structural Characterizations of 6-R-*arachno*-6,8,9-$PC_2B_7H_{11}$ (1) and 6-R-*arachno*-6,5,7-$PC_2B_7H_{11}$ (2). The 10-vertex phosphadicarbaboranes 6-R-*arachno*-6,8,9-$PC_2B_7H_{11}$ (**1a** and **1b**) and 6-R-*arachno*-6,5,7-$PC_2B_7H_{11}$ (**2a** and **2b**) were respectively synthesized by reactions of the isomeric adjacent-carbon *arachno*-4,5-$C_2B_7H_{13}$[5] and nonadjacent-carbon *arachno*-4,6-$C_2B_7H_{13}$[6] carboranes with $RPCl_2$ (R = Ph, **1a** and **2a**; R = Me, **1b** and **2b**) in the presence of Proton Sponge (eqs 1 and 2).

$$\textit{arachno}\text{-}4,5\text{-}C_2B_7H_{13} + RPCl_2 \xrightarrow[-3\ PSH^+Cl^-]{\text{(1) 3 PS; (2) xs HCl}} 6\text{-R-}\textit{arachno}\text{-}6,8,9\text{-}PC_2B_7H_{11} \quad (1)$$
(R = Ph, **1a**; Me, **1b**)

$$\textit{arachno}\text{-}4,6\text{-}C_2B_7H_{13} + RPCl_2 \xrightarrow[-2\ PSH^+Cl^-]{2\ PS} 6\text{-R-}\textit{arachno}\text{-}6,5,7\text{-}PC_2B_7H_{11} \quad (2)$$
(R = Ph, **2a**; Me, **2b**)

The products were isolated as air- and moisture-sensitive materials with typical yields ranging from 49 to 68%. The compositions of these compounds were confirmed by elemental analyses and/or high-resolution mass spectrometry.

(7) Crystal Structure Analysis Package, Molecular Structure Corporation 1985, 1992.
(8) REQAB: Jacobsen, R. A. Private communication, 1994.
(9) TwinSolve: Christer Swensson, MaxLab, Lund, Sweden, private communication.
(10) SIR92: Altomare, A.; Burla, M. C.; Camalli, M.; Cascarano, M.; Giacovazzo, C.; Guagliardi, A.; Polidoro, G. *J. Appl. Crystallogr.* **1994**, *27*, 435.
(11) Parthasrathi, V.; Beurskens, P. T.; Slot, H. J. B. *Acta Crystallogr.* **1983**, *A39*, 860−864.
(12) Sheldrick, G. M. *SHELXL-93: Program for the Refinement of Crystal Structures*; University of Göttingen: Germany, 1993.
(13) Yang, X.; Jiao, H.; Schleyer, P. v. R. *Inorg. Chem.* **1997**, *36*, 4897−4899 and references therein.
(14) Frisch, M, J.; Trucks, G. W.; Schlegel, H. B.; Gill, P. M. W.; Johnson, B. G.; Robb, M. A.; Cheeseman, J. R.; Keith, T.; Peterson, G. A.; Montgomery, J. A.; Raghavachari, K.; Al-Laham, M. A.; Zakrzewski, V. G.; Ortiz, J. V.; Foresman, J. B.; Cioslowski, J.; Stefanov, B. B.; Nanayakkara, A.; Challacombe, M.; Peng, C. Y.; Ayala, P. Y.; Chen, W.; Wong, M. W.; Andres, J. L.; Replogle, E. S.; Gomperts, R.; Martin, R. L.; Fox, D. J.; Binkley, J. S.; Defrees, D. J.; Baker, J.; Stewart, J. P.; Head-Gordon, M.; Gonzalez, C.; Pople, J. A. *Gaussian 94*, revision E.2; Gaussian, Inc.: Pittsburgh, PA, 1995.
(15) Frisch, M, J.; Trucks, G. W.; Schlegel, H. B.; Scuseria, G. E.; Robb, M. A.; Cheeseman, J. R.; Zakrzewski, V. G.; Montgomery, J. A., Jr.; Stratmann, R. E.; Burant, J. C.; Dapprich, S.; Millam, J. M.; Daniels, A. D.; Kudin, K. N.; Strain, M. C.; Farkas, O.; Tomasi, J.; Barone, V.; Cossi, M.; Cammi, R.; Mennucci, B.; Pomelli, C.; Adamo, C.; Clifford, S.; Ochterski, J.; Petersson, G. A.; Ayala, P. Y.; Cui, Q.; Morokuma, K.; Malick, D. K.; Rabuck, A. D.; Raghavachari, K.; Foresman, J. B.; Cioslowski, J.; Ortiz, J. V.; Baboul, A. G.; Stefanov, B. B.; Liu, G.; Liashenko, A.; Piskorz, P.; Komaromi, I.; Gomperts, R.; Martin, R. L.; Fox, D. J.; Keith, T.; Al-Laham, M. A.; Peng, C. Y.; Nanayakkara, A.; Challacombe, M.; Gill, P. M. W.; Johnson, B.; Chen, W.; Wong, M. W.; Andres, J. L.; Gonzalez, C.; Head-Gordon, M.; Replogle, E. S.; Pople, J. A. *Gaussian 98*, revision A.9; Gaussian, Inc.: Pittsburgh, PA, 1998.
(16) (a) Bausch, J. W.; Rizzo, R. C.; Sneddon, L. G.; Wille, A. E.; Williams, R. E. *Inorg. Chem.* **1996**, *35*, 131−135. (b) Shedlow, A. M.; Sneddon, L. G. *Inorg. Chem.* **1998**, *37*, 5269−5277. (c) Kadlecek, D. E.; Carroll, P. J.; Sneddon, L. G. *J. Am. Chem. Soc.* **2000**, *122*, 10868−10877.
(17) Tebben, A. J. M.S. Thesis, Villanova University, 1997.

Table 3. Crystallographic Data Collection and Structure Refinement Information

	1a	**2a**	**7**	**8**
empirical formula	$C_8B_7H_{16}P$	$C_8B_7H_{16}P$	$Pt_2C_{35}B_{28}H_{67}P_4Br_4$	$PdC_{16}B_{14}H_{32}P_2Br_2$
formula weight	218.85	218.85	1624.27	703.92
crystal class	orthorhombic	triclinic	triclinic	monoclinic
space group	*Pbca*	$P\bar{1}$	$P\bar{1}$	$P2_1/n$ (#14)
Z	8	4	2	2
a, Å	12.5579(1)	11.0280(2)	15.5744(3)	8.6301(7)
b, Å	15.6169(2)	11.0406(3)	18.3360(3)	8.5428(7)
c, Å	12.6071(1)	10.7862(2)	11.3806(2)	19.166(2)
α, deg		107.620(1)	102.285(1)	
β, deg		91.338(2)	109.983(1)	92.095(3)
γ, deg		95.646(1)	78.590(1)	
V, Å^3	2472.45(4)	1243.64(5)	2956.54(9)	1412.1(2)
μ, cm^{-1}	1.81	1.80	75.68	36.08
crystal size, mm^3	0.32 × 0.30 × 0.26	0.23 × 0.15 × 0.14	0.26 × 0.20 × 0.06	0.32 × 0.12 × 0.06
D_{calc}, g/cm^3	1.176	1.169	1.825	1.656
F(000)	912	456	1546	688
2*θ* angle, deg	5.22−50.68	5.08−50.7	5.04−54.96	5.1−55.1
hkl collected	$-15 \le h \le 15$	$-13 \le h \le 13$	$-20 \le h \le 20$	$-10 \le h \le 10$
	$-18 \le k \le 18$	$-13 \le k \le 13$	$-23 \le k \le 23$	$-10 \le k \le 10$
	$-15 \le l \le 15$	$-12 \le l \le 12$	$-14 \le l \le 14$	$-21 \le l \le 23$
no. of reflns measured	13 524	10 088	30 754	8710
no. of unique reflns	2257 (R_{int} = 0.0393)	4190 (R_{int} = 0.0296)	12 376 (R_{int} = 0.0515)	8710
no. of observed reflns	2129 ($F > 4\sigma$)	3781 ($F > 4\sigma$)	11 206 ($F > 4\sigma$)	8221 ($F > 4\sigma$)
no. of reflns used in refinement	2257	4190	12 376	8710
no. parameters	213	417	659	161
R^a indices ($F > 4\sigma$)	R_1 = 0.0685	R_1 = 0.0485	R_1 = 0.0550	R_1 = 0.0852
	wR_2 = 0.1519	wR_2 = 0.1080	wR_2 = 0.1407	wR_2 = 0.2261
R^a indices (all data)	R_1 = 0.0740	R_1 = 0.0553	R_1 = 0.0614	R_1 = 0.0898
	wR_2 = 0.1548	wR_2 = 0.1123	wR_2 = 0.1476	wR_2 = 0.2320
GOF ^{b}	1.316	1.102	1.130	1.217
final difference peaks, e/Å^3	+0.200, −0.215	+0.186, −0.296	+1.912, −2.278	+4.315, −1.811

	9	**10**	**11**
empirical formula	$PtC_{53}B_7H_{53}P_3$	$CoC_{13}B_7H_{19}P$	$NiC_{16}B_{14}H_{28}P_2$
formula weight	1053.62	340.85	492.37
crystal class	triclinic	orthorhombic	monoclinic
space group	$P\bar{1}$	*Pbcn*	$P2_1/c$
Z	2	8	4
a, Å	12.9520(3)	23.4553(2)	13.0466(2)
b, Å	18.3819(4)	7.9746(1)	10.5141(2)
c, Å	11.2556(3)	17.2053(2)	17.7492(2)
α, deg	92.702(2)		
β, deg	114.316(1)		90.271(1)
γ, deg	81.214(2)		
V, Å^3	2413.01(10)	3218.19(6)	2434.69(7)
μ, cm^{-1}	30.43	11.50	9.34
crystal size, mm^3	0.32 × 0.22 × 0.07	0.32 × 0.25 × 0.08	0.42 × 0.26 × 0.24
D_{calc}, g/cm^3	1.450	1.407	1.343
F(000)	1058	1392	1008
2*θ* angle, deg	5.26−54.96	5.04−50.7	5.48−50.68
hkl collected	$-16 \le h \le 15$	$-25 \le h \le 28$	$-15 \le h \le 15$
	$-23 \le k \le 23$	$-9 \le k \le 9$	$-12 \le k \le 12$
	$-14 \le l \le 14$	$-20 \le l \le 18$	$-21 \le l \le 20$
no. of reflns measured	25 744	18 897	19 738
no. of unique reflns	10 157 (R_{int} = 0.0382)	2940 (R_{int} = 0.0352)	4230 (R_{int} = 0.0284)
no. of observed reflns	9610 ($F > 4\sigma$)	2829 ($F > 4\sigma$)	4080 ($F > 4\sigma$)
no. of reflns used in refinement	10 157	2940	4230
no. parameters	614	266	410
R^a indices ($F > 4\sigma$)	R_1 = 0.0499	R_1 = 0.0373	R_1 = 0.0361
	wR_2 = 0.1372	wR_2 = 0.0873	wR_2 = 0.0897
R^a indices (all data)	R_1 = 0.0527	R_1 = 0.0398	R_1 = 0.0379
	wR_2 = 0.1425	wR_2 = 0.0889	wR_2 = 0.0909
GOF ^{b}	1.113	1.180	1.090
final difference peaks, e/Å^3	+1.956, −2.061	+0.302, −0.308	+0.255, −0.462

^{a} $R_1 = \sum||F_o| - |F_c||/\sum|F_o|$; $wR_2 = \{\sum w(F_o^2 - F_c^2)^2/\sum w(F_o^2)^2\}^{1/2}$. ^{b} GOF = $\{\sum w(F_o^2 - F_c^2)^2/(n - p)\}^{1/2}$, where n = no. of reflections and p = no. of parameters refined.

If, as in other phosphapolyboranes,[1,18] the RP unit is a four-electron donor to the cage, then **1** and **2** each have 26 skeletal electrons and should adopt a 10-vertex *arachno*-geometry ($n + 3$ skeletal electron pairs),[19] based on an icosahedron minus two vertexes. As diagramed in Figure 1, depending on how insertion of the RP unit into the skeletal framework of the *arachno*-4,5-$C_2B_7H_{13}$ and *arachno*-4,6-$C_2B_7H_{13}$ occurs,

(18) (a) Getman, T. D.; Deng, H.-B.; Hsu, L.-Y.; Shore, S. G. *Inorg. Chem.* **1989**, *28*, 3612−3616. (b) Jutzi, P.; Wegener, D.; Hursthouse, M. *J. Organomet. Chem.* **1991**, *418*, 277−289.

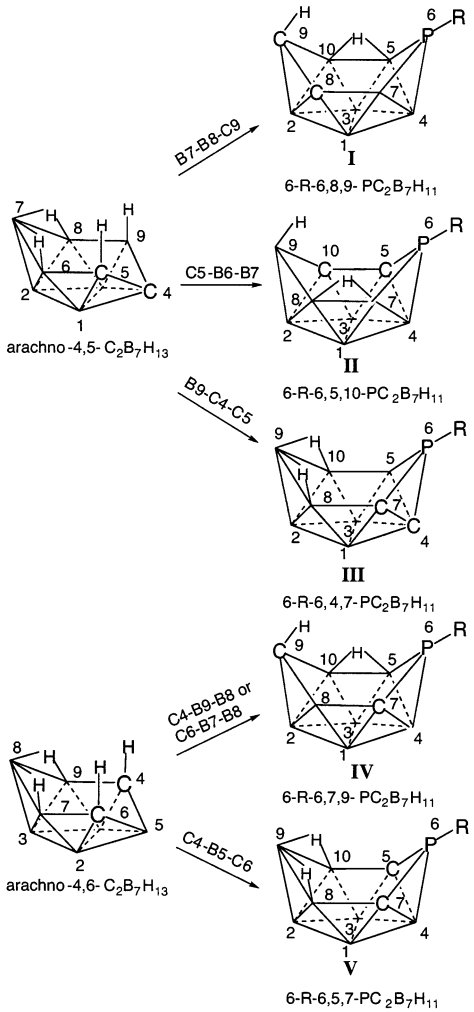

Figure 1. Possible geometric isomers of 6-R-*arachno*-$PC_2B_7H_{11}$ derived from *arachno*-4,5-$C_2B_7H_{13}$ and *arachno*-4,6-$C_2B_7H_{13}$.

a number of different geometric isomers could result. Thus, for the *arachno*-4,5-$C_2B_7H_{13}$ carborane, three isomers are possible resulting from insertion at the B7−B8−B9, C5−B6−B7, or B9−C4−C5 positions to respectively yield the 6-R-*arachno*-6,8,9-$PC_2B_7H_{11}$ (**I**), 6-R-*arachno*-6,5,10-$PC_2B_7H_{11}$ (**II**), or 6-R-*arachno*-6,4,7-$PC_2B_7H_{11}$ (**III**) isomers. Because of the C_s symmetry of the *arachno*-4,6-$C_2B_7H_{13}$ carborane, only two isomeric products are possible. Thus, insertion at either C6−B7−B8 or B8−B9−C4 yields the two enantiomeric forms of the same 6-R-*arachno*-6,7,9-$PC_2B_7H_{11}$ geometric isomer (**IV**), whereas insertion at the position spanning C4−B5−C6 yields the C_s-symmetric 6-R-*arachno*-6,5,7-$PC_2B_7H_{11}$ (**V**).

Density functional theory (DFT) calculations at the B3LYP/6-311G* level for the five isomers yielded the optimized molecular geometries shown in Figure 2. The 6-Me-*arachno*-6,8,9-$PC_2B_7H_{11}$ (**I**) structure is of lowest energy, in agreement with the known tendency of electron-rich heteroatoms, such as phosphorus and carbon, to favor the lowest-coordinate positions (i.e., the 6- and 9-position) on the open face of a polyhedral framework.[16a,20] Only slightly higher in energy (0.2 kcal/mol) is the 6-Me-*arachno*-6,7,9-$PC_2B_7H_{11}$ isomer (**IV**), which also has the phosphorus and one carbon located in the low-coordinate 6- and 9-position but has the second carbon in the facial 7-position adjacent to the phosphorus rather than the carbon-adjacent 8-position in **I**. In the 6-Me-*arachno*-6,5,10-$PC_2B_7H_{11}$ (**II**) and 6-Me-*arachno*-6,5,7-$PC_2B_7H_{11}$ (**V**) isomers, the phosphorus is again in the 6-position, but the carbon atoms in each compound are located in unfavorable higher-coordinate positions (C5, C10 and C5, C7, respectively). The higher energy of the **V** structure (17.4 kcal/mol), where P6 is connected to two carbons and one boron, compared to that of **II** (16.6 kcal/mol), where P6 is connected to two borons and one carbon, is consistent with the tendency of the most electron-rich heteroatoms in a cage to favor bonding interactions with electron-poor neighbors.[16a,20] As expected based on the unfavorable location of one of the carbons in the high-coordinate 4-position of the cage skeleton, the 6-R-*arachno*-6,4,7-$PC_2B_7H_{11}$ (**III**) isomer was found to be of highest energy (29.5 kcal/mol).

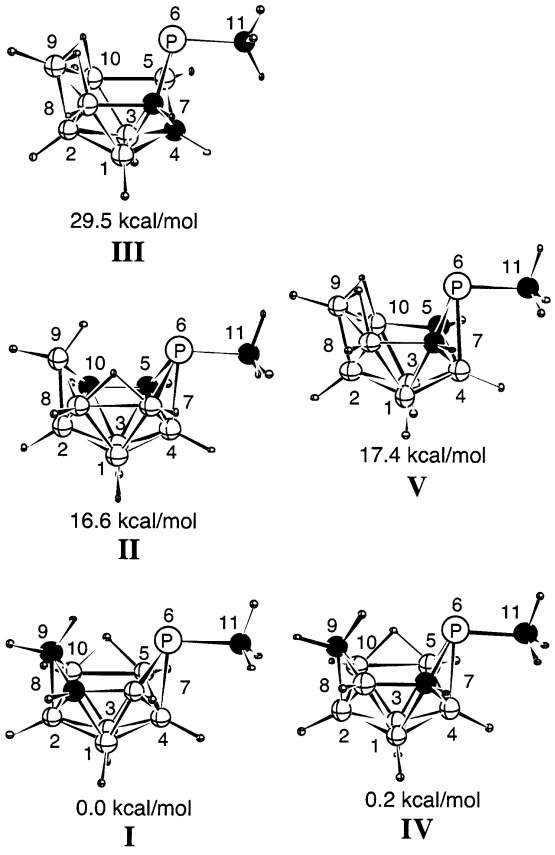

Figure 2. DFT calculated optimized geometries and relative energies for isomeric 6-R-*arachno*-$PC_2B_7H_{11}$ structures.

Single-crystal X-ray diffraction determinations (Figure 3a and b) established that compound **1a** adopts the thermodynamically favored 6-Ph-*arachno*-6,8,9-$PC_2B_7H_{11}$ structure (Ph derivative of **I**), while **2a** adopts the higher energy 6-Ph-*arachno*-6,5,7-$PC_2B_7H_{11}$ structure (Ph derivative of **V**). The phosphorus atoms in both compounds are located in the low-coordinate 6-position, but the carbon and the bridge and/or *endo*-hydrogen atoms in the two isomers are found in different locations. In **1a**, one carbon is present in the favored low-coordinate 9-position, while

(19) (a) Williams, R. E. *Inorg. Chem.* **1971**, *10*, 210−214. (b) Wade, K. *Adv. Inorg. Chem. Radiochem.* **1976**, *18*, 1−66. (c) Williams, R. E. *Chem. Rev.* **1992**, *92*, 177−207. (d) Rudolph, R. W.; Thompson, D. A. *Inorg. Chem.* **1974**, *13*, 2779−2782. (d) Williams, R. E. In *Electron Deficient Boron and Carbon Clusters*; Olah, G. A., Wade, K., Williams, R. E., Eds.; Wiley: New York, 1991; pp 11−93.

(20) Williams, R. E. *Adv. Inorg. Chem. Radiochem.* **1976**, *18*, 67−142.

the other carbon is found in the adjacent higher-coordinate 8-position. There is an *endo*-hydrogen at the C9 carbon and a hydrogen bridging the B5−B10 edge. In **2a**, the two carbons are nonadjacent and are situated in the higher-coordinate cage positions adjacent to the phosphorus, with bridge-hydrogens present at the B9−B8 and B9−B10 edges. The observed bond distances and angles fall into the normal ranges; however, there are some differences between the two compounds that can be related to their different donor properties. As discussed later, in contrast to **1a**, **2a** shows donor properties consistent with a lone pair of electrons localized at the *endo*-P6 position. Consistent with this observation, the B4−P6−C11 (87.04(10)°), C5−P6−C11 (106.44(11)°), C7−P6−C11 (105.08(10)°), and C5−P6−C7 (86.18(10)°) bond angles in **2a** are considerably more acute than the comparable B4−P6−C11 (97.50(13)°), B5−P6−C11 (113.05(14)°), B7−P6−C11 (113.6(2)°), and B5−P6−B7 (95.7(2)°) angles in **1a**, suggesting that in **2a** the P6−C11 bond is being repelled by the P6 lone pair. In **2a**, the P6−C11 (1.839(2) Å) and P6−B4 (2.208(3) Å) bond distances are also significantly longer than the comparable distances in **1a** (P6−C11 (1.820(3) Å) and P6−B4 (2.050(3) Å) probably as a result of the shorter P6−C5 (1.885(2) Å) and P6−C7 (1.888(2) Å) bonds in **2a** relative to the P6−B5 (1.986(4) Å) and P6−B7 (1.984(4) Å) bonds in **1a**.

The spectroscopic properties for compounds **1a,b** and **2a,b** are consistent with both the crystallographically determined structures and with the results of the DFT/GIAO chemical shift calculations (Table 1). Thus, the ^{11}B NMR spectral patterns of **1a,b** indicate C_1 cage-symmetry, while those of **2a,b** indicate C_S symmetry, with the DFT/GIAO calculated values and assignments for structures **I** and **V** closely matching those experimentally determined in the two-dimensional COSY ^{11}B−^{11}B NMR studies of **1a** and **2a** (Table 1). Likewise, in the **1a** ^{11}B NMR spectra, the resonances near −12 and −20 ppm clearly show bridge-hydrogen couplings consistent with their calculated assignments to the B5 and B10 borons.

In addition to their respective Ph or Me resonances, the ^{1}H NMR spectra of **1a** and **1b** show the expected seven terminal BH, an intensity-one bridge-hydrogen, and three cage-CH resonances with one of the cage-CH resonances in both compounds occurring at the high field (−0.72 ppm, **1a**; −0.90 ppm, **1b**) characteristic of an *endo*-hydrogen of a cage-CH_2 group.[21] The ^{1}H NMR spectra of **2a** and 2**b** showed, in addition to their terminal BH and respective phenyl or methyl resonances, intensity-two bridge-hydrogen and cage-CH resonances.

The calculated ^{13}C and ^{31}P chemical shifts for **I** and **V** (and their Ph-analogues) match well with the experimentally determined values for **1a,b** and **2a,b**. The $J_{^{13}C-^{31}P}$ values observed in these compounds deserve special comment. The room temperature ^{1}H-decoupled ^{13}C NMR spectra of **2a,b** contained a single resonance with a multiplet structure arising from both boron and phosphorus coupling. When the temperature was lowered to −83°C to thermally decouple ^{11}B interactions,[22] this resonance resolved into a sharp doublet with the magnitude of the phosphorus−carbon coupling ($J_{^{13}C-^{31}P}$ 55 Hz, **2a** and 52 Hz, **2b**) being consistent with the adjacent positions of the carbon (C5,7) and phosphorus (P6) atoms. The ^{13}C NMR spectra of **1a** and **1b** showed the expected two cage-carbon resonances, one of which appeared as a triplet of doublets and the other as a doublet, consistent with the C9−H_2 and C8−H cage units, respectively. Surprisingly, given its location on the opposite side of the cage from the P6 atom, the C9-carbon exhibited significant carbon−phosphorus coupling ($J_{^{13}C-^{31}P}$ 49 Hz, **1a** and 43 Hz, **1b**). These values are close to normal $^2J_{CP}$ or $^1J_{CP}$ coupling values,[23] such as discussed above for the $^1J_{CP}$ coupling value found for phosphorus-adjacent C5,7-carbons in compounds **2a,b**. An examination of the crystallographically determined structure of **1a** shown in Figure 3 reveals that the P6−H9 distance (2.49(4) Å) is shorter that the van der Waals radii of phosphorus and hydrogen (3.1 Å). As shown in Figure 4a, DFT calculations on **Ia** also showed that there is significant interaction of electrons localized at the *endo*-P6 position and the *endo*-C9−H hydrogen in the HOMO. This suggests an intramolecular C9−H9−P6 hydrogen-bonding interaction in **1a,b** as the mechanism for the $J_{^{13}C9-^{31}P6}$ coupling observed in the ^{13}C NMR spectra of these compounds.

When the progress of the reaction given in eq 2 was monitored by ^{11}B NMR spectroscopy, no intermediate species were observed. However, when the reaction in eq 1 leading to **1a** was monitored, an intermediate anionic species was observed after addition of $PhPCl_2$ and excess Proton Sponge. The ^{11}B NMR spectrum of this intermediate anion is in good agreement

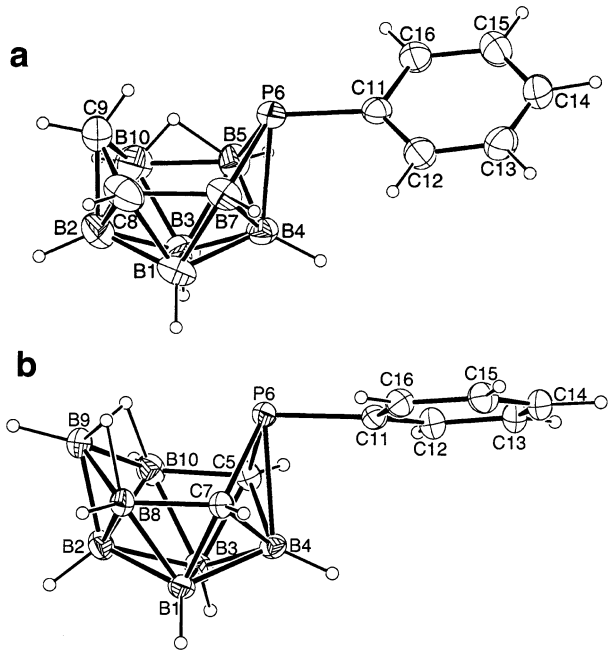

Figure 3. (a) ORTEP drawing of 6-Ph-*arachno*-6,8,9-$PC_2B_7H_{11}$ (**1a**). Selected bond distances (Å) and angles (deg): B5−P6, 1.986(4); P6−B7, 1.984(4); B7−C8, 1.721(6); C8−C9, 1.660(8); C9−B10, 1.660(7); B10−B5, 1.714(5); P6−C11, 1.820(3); P6−B4, 2.050(3); B4−P6−C11, 97.50(13); B5−P6−C11, 113.05(14); B7−P6−C11, 113.6(2); B5−P6−B7, 95.7(2). (b) ORTEP drawing of 6-Ph-*arachno*-6,5,7-$PC_2B_7H_{11}$ (**2a**). Selected bond distances (Å) and angles (deg): C5−P6, 1.885(2); P6−C7, 1.888(2); C7−B8, 1.635(4); B8−B9, 1.825(5); B9−B10, 1.830(5); B10−C5; 1.636(4); P6−C11, 1.839(2); P6−B4, 2.208(3); B4−P6−C11, 87.04(10); C5−P6−C11, 106.44(11); C7−P6−C11, 105.08(10); C5−P6−C7, 86.18(10).

(21) Kang, S. O.; Furst, G. T.; Sneddon, L. G. *Inorg. Chem.* **1989**, *28*, 2339−2347 and references therein.

(22) (a) Wrackmeyer, B. In *Progress in NMR Spectroscopy*; Emsley, J. W., Feeney, J., Sutcliffe, L. H., Eds.; Pergamon: New York, 1979; Vol. 12, pp 227−259. (b) Gragg, B. R.; Layton, W. J.; Niedenzu, K. *J. Organomet. Chem.* **1977**, *132*, 29−36.

(23) Quin, L. D. In *Phosphorus-31 NMR Spectroscopy in Stereochemical Anaylsis*; Verkade, J. G.; Quin, L. D., Eds.; VCH: New York, 1987; Chapter 12.

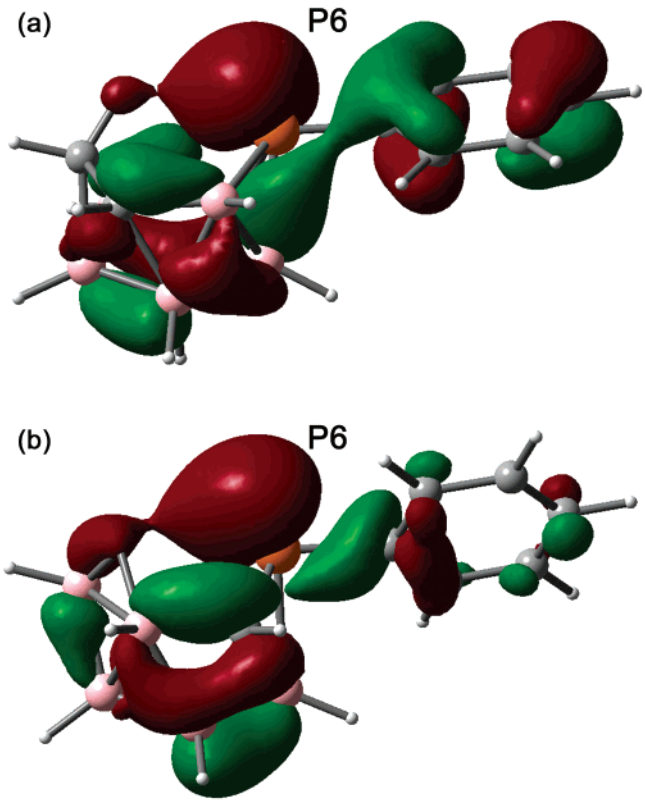

Figure 4. HOMO density surfaces for (a) 6-Ph-*arachno*-6,8,9-$PC_2B_7H_{11}$ (**Ia**) and (b) 6-Ph-*arachno*-6,5,7-$PC_2B_7H_{11}$ (**Va**).

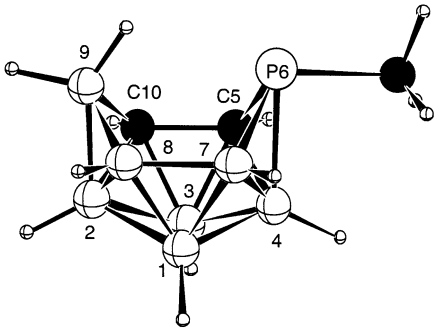

Figure 5. DFT optimized geometry $\mathbf{II}^-$ for the 6-R-*arachno*-6,5,10-$PC_2B_7H_{10}^-$ anion. Selected bond distances (Å) and angles (deg): P6−B4, 2.162; C5−P6, 1.891; P6−B7, 2.015; P6−C11, 1.904; C5−C10, 1.526; C5−P6−B7, 90.1; B4−P6−C11, 88.1; C5−P6−C11, 102.9; B7−P6−C11, 112.7.

with the DFT/GIAO calculated chemical shifts (Table 1) for that of the 6-R-*arachno*-6,5,10-$PC_2B_7H_{10}^-$ anion ($\mathbf{II}^-$, Figure 5). Protonation of this anion would then be expected to produce neutral 6-R-*arachno*-6,5,10-$PC_2B_7H_{11}$ having structure **II** shown in Figure 2. However, owing to its unfavorable carbon locations, **II** is 16.6 kcal/mol higher in energy than **I**, and indeed, it was found that when the intermediate 6-R-*arachno*-6,5,10-$PC_2B_7H_{10}^-$ (with structure $\mathbf{II}^-$) was protonated with $HCl{\cdot}OEt_2$, 6-R-*arachno*-6,8,9-$PC_2B_7H_{11}$ (**1**) with structure **I**, rather than **II**, was produced.

The formation of the structures established for 6-R-*arachno*-6,8,9-$PC_2B_7H_{11}$ (**1**, Figure 3a) and 6-R-*arachno*-6,5,7-PC_2B_7-H11 (**2**, Figure 3b) by the reactions given in eqs 1 and 2 can be envisioned to have resulted from a series of substitution/dehydrohalogenation steps.[16b] Initial deprotonation of *arachno*-4,5-$C_2B_7H_{13}$ has been shown to occur at the *endo*-C5−H.[24]

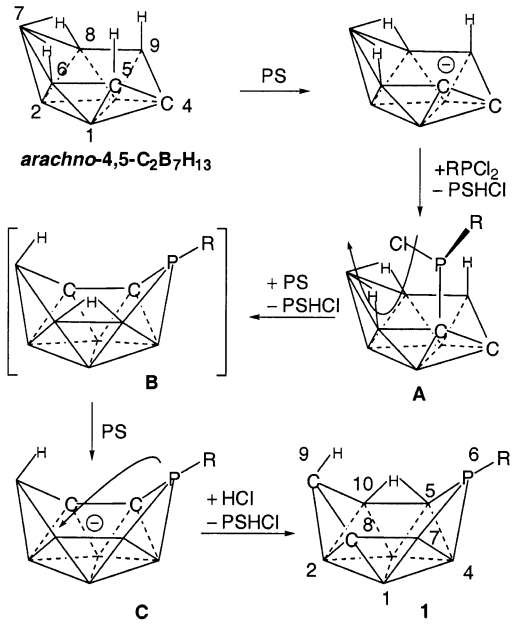

Figure 6. Possible reaction steps leading to the formation of 6-R-*arachno*-6,8,9-$PC_2B_7H_{11}$ (**1**).

Reaction of the resulting *arachno*-4,5-$C_2B_7H_{12}^-$ anion with $RPCl_2$ would then reasonably result in the formation of 5-RPCl-*arachno*-4,5-$C_2B_7H_{12}$ (**A**, Figure 6), in which the RPCl− group is substituted at C5. A subsequent B6−B7 bridge-hydrogen deprotonation−dehydrohalogenation involving a second equivalent of Proton Sponge would result in phosphorus cage insertion to yield **B**, which, in the presence of the of excess Proton Sponge, would deprotonate to the 6-R-*arachno*-6,5,10-$PC_2B_7H_{10}^-$ anion (**C**) (having structure $\mathbf{II}^-$) that was observed by ^{11}B NMR spectroscopy. Acidification of **C** ($\mathbf{II}^-$) then results in cage rearrangement to generate the final product **1** (with structure **I**).

Deprotonation of the *arachno*-4,6-$C_2B_7H_{13}$ carborane has also been previously shown to occur at the *endo*-C4−H to produce the *arachno*-4,6-$C_2B_7H_{12}^-$ anion having the negative charge largely localized on the C4 carbon.[25] A metathesis reaction of this anion with $RPCl_2$ could then yield a 4-RPCl-*arachno*-4,6-$C_2B_7H_{12}$ derivative **D** (Figure 7). Deprotonation of the acidic *endo*-C6−H of **D** by an additional equivalent of Proton Sponge, followed by dehydrohalogenation, then leads in a straightforward manner to the structure (**V**) observed for 6-R-*arachno*-6,5,7-$PC_2B_7H_{11}$ (**2**) having the phosphorus inserted between the two carbons.

Even though the DFT calculations show that structure **V** is considerably higher in energy, the isomerization of **2** to **1** (with the more stable structure **I**) was not observed even after being heated at 90 °C in DME for 2 days.

Reactions of 6-R-*arachno*-6,8,9-$PC_2B_7H_{11}$ (1) and 6-R-*arachno*-6,5,7-$PC_2B_7H_{11}$ (2) with $BH_3{\cdot}THF$, S_8, and H_2O_2. The insertion of electron-rich elements, such as phosphorus, into a boron cluster normally results in the formation of a compound having a formal lone pair of electrons associated with the heteroatom. Because of the extensive electron delocalization in

(24) Jelìnek, T.; Holub, J.; Stíbr, B.; Fontaine, X. L. R.; Kennedy, J. D. *Collect. Czech. Chem. Commun.* **1994**, *59*, 1584−1595.
(25) (a) Tebbe, F. N.; Garrett, P. M.; Hawthorne, M. F. *J. Am. Chem. Soc.* **1968**, *90*, 869−879. (b) Kadlecek, D. E.; Hong, D.; Carroll, P. J.; Sneddon, L. G. In preparation.

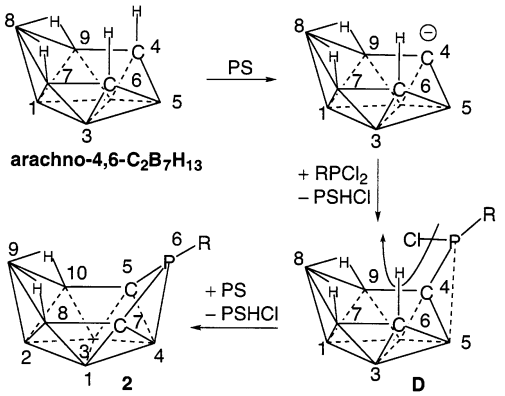

Figure 7. Possible reaction steps leading to the formation of 6-R-*arachno*-6,5,7-$PC_2B_7H_{11}$ (**2**).

polyhedral boron clusters, these heteroatom lone pairs are usually delocalized and have low Lewis basicity.[1] However, we have recently found that the 10-vertex phosphamonocarbaborane anion *exo*-6-R-*arachno*-6,7-$PCB_8H_{11}^-$ shows strong donor properties arising from a phosphorus-localized lone pair of electrons.[2] The 6-R-*arachno*-6,8,9-$PC_2B_7H_{11}$ (**1**) and 6-R-*arachno*-6,5,7-$PC_2B_7H_{11}$ (**2**) phosphadicarbaboranes are isoelectronic with the *exo*-6-R-*arachno*-6,7-$PCB_8H_{11}^-$ anion and have similar 10-vertex *arachno*-structures in which their phosphorus atoms occupy the 6-position in the cage. DFT calculations on the HOMO density surfaces (Figure 4) revealed that both **Ia** (**1a**) and **Va** (**2a**) have significant electron density localized at their *endo*-phosphorus positions. These observations prompted our investigations of the reactions of **1a** and **2a** with Lewis acids to see if they would exhibit donor properties.

It was found that **1a** does not react with BH_3·THF, but when **2a** was mixed with BH_3·THF in THF, an equilibrium mixture containing both **2a** and *endo*-6-H_3B-*exo*-6-Ph-*arachno*-6,5,7-$PC_2B_7H_{11}$ (**3**) was immediately established (eq 3).

$$\underset{\textbf{2a}}{\text{6-Ph-}\textit{arachno}\text{-6,5,7-}PC_2B_7H_{11}} + BH_3\cdot THF \overset{-THF}{\rightleftharpoons} \underset{\textbf{3}}{\textit{endo}\text{-6-}H_3B\text{-}\textit{exo}\text{-6-Ph-}\textit{arachno}\text{-6,5,7-}PC_2B_7H_{11}} \quad (3)$$

3 could not be isolated in a pure form since, upon vacuum removal of solvent, complete dissociation of the BH_3 occurred and only free **2a** was observed. However, Figure 8 shows a ^{1}H-decoupled ^{11}B NMR spectrum taken for the reaction of **2a** and BH_3·THF where the peaks of free **2a** (▽) and the new **3** (●) are marked accordingly. The GIAO calculated shifts for the DFT optimized geometry **VI** shown in Figure 9a with the BH_3 bound at the *endo*-P6 position are in excellent agreement with the ^{11}B NMR spectrum observed for **3**. Although the relative ratio of **3** to **2a** increased as the amount of initial BH_3·THF was increased, complete formation of **3** could not be reached even in the presence of a large excess of BH_3·THF. Based on integrations of the relative peak intensities of the −21.6 ppm peak of **3** and the −33.0 ppm peak of **2a** in a series of equilibrium mixtures of **2a**, **3**, and BH_3·THF (Table 2), the equilibrium constant K_{eq} was obtained as ∼4 at room temperature in THF solution ($K_{eq} = [\mathbf{3}]/[\mathbf{2a}][BH_3\cdot THF]$), and ΔG was crudely estimated as −3 kJ/mol.

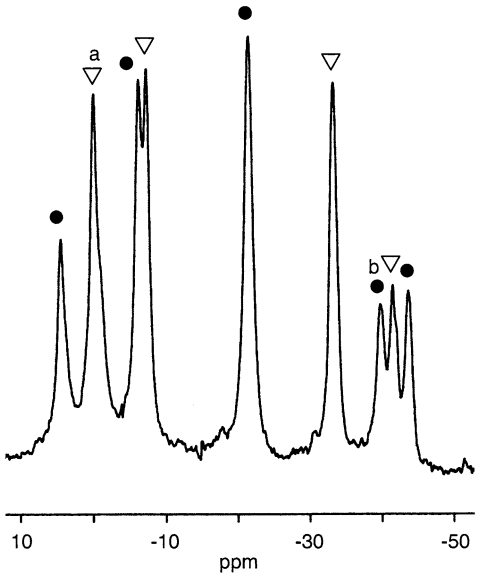

Figure 8. $^{11}B\{^1H\}$ NMR spectrum (64.2 MHz) for the reaction of **2a** with BH_3·THF, with species marked as **3** (●); **2a** (▽); BH_3·THF (a); and BH_3 group of **3** (b).

The calculated P6−BH_3 bond distance in **3** of 1.959 Å is longer than that found for $Ph_3P\cdot BH_3$ (1.93(1) and 1.90(2) Å)[26] but shorter than the corresponding P−BH_3 distance of 1.988 Å calculated for *endo*-6-BH_3-*exo*-6-Ph-*arachno*-6,7-$PCB_8H_{11}^-$.[2a]

As mentioned above, in addition to forming a complex with BH_3, the *exo*-6-R-*arachno*-6,7-$PCB_8H_{11}^-$ anion was found to react with S_8 and O_2 to form the *endo*-6-S-*exo*-6-Ph-*arachno*-6,7-$PCB_8H_{11}^-$ and *endo*-6-O-*exo*-6-Ph-*arachno*-6,7-$PCB_8H_{11}^-$ adducts.[2a] In contrast, the 6-Ph-*arachno*-6,8,9-$PC_2B_7H_{11}$ (**1a**) did not react with S_8 and was completely decomposed to borates by hydrogen peroxide. However, in its reactions with S_8 and hydrogen peroxide, 6-Ph-*arachno*-6,5,7-$PC_2B_7H_{11}$ (**2a**) formed *endo*-6-S-*exo*-6-Ph-*arachno*-6,5,7-$PC_2B_7H_{11}$ (**4**, eq 4) and *endo*-6-O-*exo*-6-Ph-*arachno*-6,5,7-$PC_2B_7H_{11}$ (**5**, eq 5).

$$\underset{\textbf{2a}}{\text{6-Ph-}\textit{arachno}\text{-6,5,7-}PC_2B_7H_{11}} \xrightarrow{1/8\,S_8} \underset{\textbf{4}}{\textit{endo}\text{-6-S-}\textit{exo}\text{-6-Ph-}\textit{arachno}\text{-6,5,7-}PC_2B_7H_{11}} \quad (4)$$

$$\underset{\textbf{2a}}{\text{6-Ph-}\textit{arachno}\text{-6,5,7-}PC_2B_7H_{11}} \xrightarrow{H_2O_2} \underset{\textbf{5}}{\textit{endo}\text{-6-O-}\textit{exo}\text{-6-Ph-}\textit{arachno}\text{-6,5,7-}PC_2B_7H_{11}} \quad (5)$$

The ^{11}B NMR spectra of **4** and **5** are quite similar, each showing five boron resonances at similar chemical shift values in 1:2:2:1:1 intensity ratios indicating C_s symmetry. The GIAO calculated chemical shifts for the DFT optimized geometries **VII** and **VIII** (Figure 9b and c) are in good accordance with the experimental data for **4** and **5** (Table 1). In both **4** (**VII**) and **5** (**VIII**), the sulfur and the oxygen atoms are located at the *endo*-P6 position with bridge-hydrogens at the B8−B9 and B9−B10 edges. The calculated values of the P6−S (1.970 Å) distance in **VII**, and the P6−O distance (1.495 Å) in **VIII** are

(26) There are two independent molecules in the unit cell; see: Huffman, J. C.; Skupinski, W. A.; Caulton, K. G. *Cryst. Struct. Commun.* **1982**, *11*, 1435−1440.

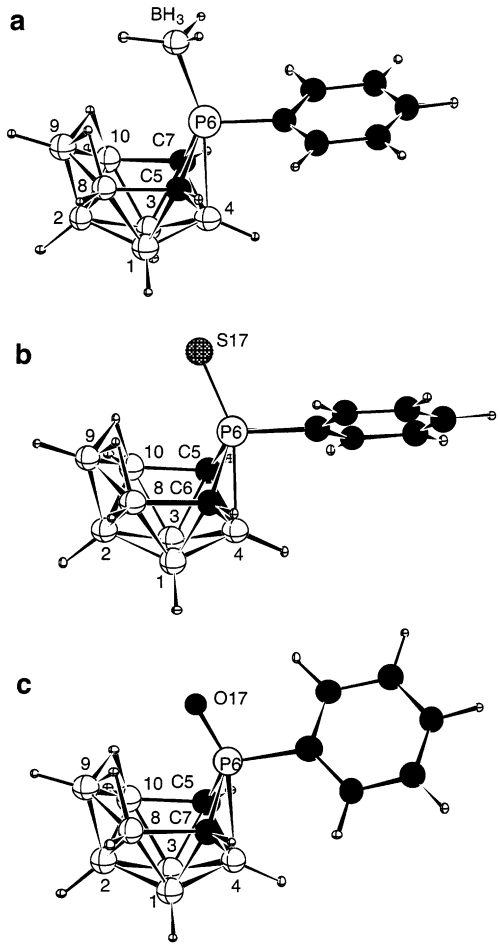

Figure 9. DFT optimized geometries: (a) **VI** for *endo*-6-BH_3-*exo*-6-Ph-*arachno*-6,5,7-$PC_2B_7H_{11}$ (**3**), (b) **VII** for *endo*-6-S-*exo*-6-Ph-*arachno*-6,5,7-$PC_2B_7H_{11}$ (**4**), and (c) **VIII** for *endo*-6-O-*exo*-6-Ph-*arachno*-6,5,7-$PC_2B_7H_{11}$ (**5**). Selected bond distances (Å) and angles (deg): (**VI**) P6−BH_3, 1.959; P6−C11, 1.838; C5−P6, 1.871; P6−C7, 1.864; C7−B8, 1.660; B8−B9, 1.810; B9−B10, 1.810; B10−C5, 1.660; P6−B4, 2.260; BH_3−P6−C11; 106.5; B4−P6−C11, 89.7; B4−P6−BH_3, 163.8; C5−P6−BH_3, 123.2; C7−P6−BH_3, 123.6; (**VII**) P6−S17, 1.970; P6−C11, 1.833; C5−P6, 1.858; P6−C7, 1.867; C7−B8, 1.680; B8−B9, 1.800; B9−B10, 1.800; B10−C5, 1.680; P6−B4, 2.280; S17−P6−C11, 109.8; B4−P6−C11, 90.7; B4−P6−S17, 159.5; C5−P6−S17, 121.6; C7−P6−S17, 121.1; (**VIII**) P6−O17, 1.495; P6−C11, 1.825; C5−P6, 1.852; P6−C7, 1.841; C7−B8, 1.690; B8−B9, 1.800; B9−B10, 1.800; B10−C5, 1.690; P6−B4, 2.282; O17−P6−C11, 109.1; B4−P6−C11, 95.8; B4−P6−O17, 155.0; C5−P6−O17, 117.9; C7−P6−O17, 120.5.

comparable to the P−S and P−O distances that have been observed in phosphine sulfides[27] and phosphine oxides,[28] respectively, but are shorter than those calculated[2a] for the analogous distances in the *endo*-6-S-*exo*-6-Ph-*arachno*-6,7-$PCB_8H_{11}^-$ (P−S, 2.030 Å) and *endo*-6-O-*exo*-6-Ph-*arachno*-6,7-$PCB_8H_{11}^-$ (P−O, 1.520 Å) compounds.

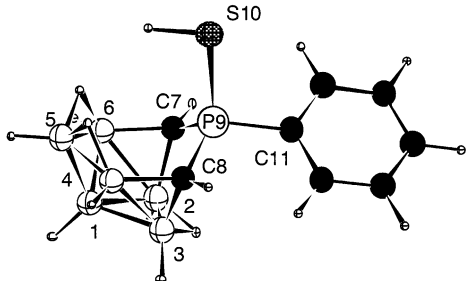

Figure 10. DFT calculated optimized geometry **IX** for $\mu_{7,8}$-{HS(Ph)P}-*hypho*-7,8-$C_2B_6H_{11}$ (**6**). Selected bond distances (Å) and angles (deg): P9−C7, 1.774; P9−C8, 1.770; P9−S10, 2.144; P9−C11, 1.823; B2−C7, 1.627; B6−C7, 1.604; B5−B6, 1.790; B5−B4, 1.790; B4−C8, 1.600; B3−C8, 1.620; C7−P9−C8, 104.3; C7−P9−S10, 114.2; C8−P9−S10, 114.6; S10−P9−C11, 100.3; B2−C7−P9, 105.5; B3−B2−C7, 107.8; B2−B3−C8, 107.6; B3−C8−P9, 105.7; B4−C8−P9, 116.4; B6−C7−P9, 117.1.

While the reaction of **2a** with 1 equiv of sulfur afforded **4**, in the presence of a large excess of S_8, **2a** yielded **6** (eq 6).

$$\underset{\textbf{2a}}{\text{6-Ph-}\textit{arachno}\text{-6,5,7-}PC_2B_7H_{11}} \xrightarrow[-B]{\text{xs } S_8} \underset{\textbf{6}}{\mu_{7,8}\text{-\{HS(Ph)P\}-}\textit{hypho}\text{-7,8-}C_2B_6H_{11}} \quad (6)$$

Compound **6** was obtained as a yellow oil in 52% yield, and its composition was established by high-resolution mass spectroscopy. In its ^{11}B NMR spectrum, **6** exhibited a C_s-symmetric pattern of four resonances in 2:1:2:1 ratios consistent with the loss of one cage-boron atom from **2a**. The resonance at −25.3 ppm showed an additional fine-structure characteristic of coupling to two bridge-hydrogens. In its ^1H NMR spectrum, **6** showed two different sets of bridge-hydrogens in a 2:1 intensity ratio with the intensity-one resonance exhibiting coupling ($^3J_{PH}$ = 35 Hz) to the phosphorus. The ^{13}C NMR spectrum of **6** showed one broad cage-carbon resonance. The single resonance observed in the ^{31}P NMR spectrum was found in a chemical shift region significantly downfield from those found for compounds **1**−**5**.

The GIAO calculated chemical shifts for the DFT optimized geometry **IX** shown in Figure 10 are in excellent agreement with the experimental NMR data for **6**. The compound has a structure related to that of **4** and can be envisioned to have been formed from structure **VII** (Figure 9) by both removal of the B4 cage atom and protonation of the *endo*-sulfur to produce the thiol group bound at the phosphorus *endo*-position of **IX** (**6**). The angles around the phosphorus are reasonably tetrahedral S10−P9−C11 (100.3°); S10−P9−C7 (114.2°); S10−P9−C8 (114.6°), and C7−P9−C8 (104.3°). The P9−C7 (1.774 Å) and P9−C8 (1.770 Å) are distances shorter than that of the *exo*-polyhedral P9−C11 (1.823 Å). The calculated P−SH distance of (2.144 Å) is longer than the P−S distance calculated in **VII** (1.970 Å), and this difference is consistent with the longer P−SH (2.077(1) Å) versus P−S (1.954(1) Å) distances observed in $Ph_2P(S)SH$.[29]

The **IX** structure established for **6** can be viewed in at least two different ways. If the phosphorus is considered as a cage atom, then the cluster would be a nine-vertex, 26 skeletal electron system (n + 4 skeleton electron pairs) and should adopt a *hypho*-type structure that can be derived from an icosahedron

(27) (a) Codding, P. W.; Kerr, K. A. *Acta Crystallogr*. **1978**, *B34*, 3785−3787. (b) Alder, M. J.; Cross, W. I.; Flower, K. R.; Pritchard, R. G. *J. Chem. Soc., Dalton Trans*. **1999**, 2563−2573. (c) Piccinni-Leopardi, C.; Germain, G.; Declercq, J. P.; Van Meerssche, M.; Robert, J. B.; Jurkschat, K. *Acta Crystallogr*. **1982**, *B38*, 2197−2199. (d) Grim, S. O.; Gilardi, R. D.; Sangokoca, S. A. *Angew. Chem., Int. Ed. Engl*. **1983**, *22*, 254−255. (e) Dreissig, V. W.; Plieth, K.; Zäske, P. *Acta Crystallogr*. **1972**, *B28*, 3473−3477.

(28) (a) Baures, P. W.; Silverton, J. V. *Acta Crystallogr*. **1990**, *C46*, 715−717. (b) Galdecki, Z.; Grochulski, P.; Luciak, B.; Wawrzak, Z.; Duax, W. L. *Acta Crystallogr*. **1984**, *C40*, 1197−1198. (c) Mikolajczyk, M.; Graczyk, P. P.; Wieczorek, M. W.; Bujacz, G. *Tetrahedron* **1992**, *48*, 4209−4230. (d) Cameron, T. S.; Dahlèn, B. *J. Chem. Soc., Perkin Trans. 2* **1975**, 1737−1751. (e) Bandoli, G.; Bortolozzo, G.; Clemente, D. A.; Croatto, U.; Panattoni, C. *J. Chem. Soc. A* **1970**, 2778−2780.

(29) Krebs, B.; Henkel, G. *Z. Anorg. Allg. Chem*. **1981**, *475*, 143−155.

by removing three vertexes. The structure in Figure 10 can be generated in this manner and is quite similar to those observed for other 9-vertex *hypho*-class compounds, including *hypho*-1-CH_2-2,5-$S_2B_6H_8$, *hypho*-2,5-$S_2B_7H_{10}^-$, *hypho*-2,5-$S_2B_7H_{11}$, and *hypho*-1-($NCCH_2$)-1,2,5-$C_3B_6H_{12}^-$.[30,31] On the other hand, given the tetrahedral configuration of the phosphorus, the HS(Ph)P unit could be considered to be a "classical" fragment bridging the C7 and C8 carbons of the $C_2B_6H_{11}$ dicarbaborane fragment. In this case, the PhP(SH) would be considered to donate three electrons to the cage by forming one normal σ-bond and one dative bond with the C7 and C8 cage carbons. The resulting 8-vertex C_2B_6-framework of the $\mu_{7,8}$-{HS(Ph)P}-*hypho*-7,8-$C_2B_6H_{11}$ cluster would have 24 skeletal electrons and should therefore adopt a *hypho*-type geometry that is derived by removing three vertexes from an octadecahedron.[19] The C_2B_6-framework proposed for **6** in Figure 10 is, in fact, entirely consistent with those found for other isoelectronic 8-vertex *hypho*-clusters, including *hypho*-$C_2B_6H_{13}^-$, *hypho*-$S_2B_6H_9^-$, and 2,3-Me_2-*hypho*-$S_2B_6H_8$.[30,32]

Coordination Chemistry of 6-Ph-*arachno*-6,5,7-$PC_2B_7H_{11}$ (2a). The reaction of **2a** and $PtBr_2$ afforded *cis*-(η^1-[6-Ph-*arachno*-6,5,7-$PC_2B_7H_{11}$])$_2PtBr_2$ (**7**, eq 7).

$$2\ \underset{\mathbf{2a}}{\text{6-Ph-}arachno\text{-6,5,7-}PC_2B_7H_{11}} + PtBr_2 \rightarrow \underset{\mathbf{7}}{cis\text{-}(\eta^1\text{-[6-Ph-}arachno\text{-6,5,7-}PC_2B_7H_{11}])_2PtBr_2} \quad (7)$$

A single-crystal X-ray diffraction study established the structure shown in Figure 11. Since there were no significant structural differences, only one of the two independent molecules is shown in the figure. The complex contains two *cis*-coordinated 6-Ph-*arachno*-6,5,7-$PC_2B_7H_{11}$ (**2a**) cages that are each bound to the platinum center in an η^1 fashion at the *endo*-position of the cage phosphorus P6. The geometry around the Pt(II) is a slightly distorted square plane, with the P−Pt−P angle (95.61(7)°) being wider than Br−Pt−Br (87.38(3)°) owing to the greater steric requirements of the bulky cages. The Pt−P bond distances (2.254(2) and 2.268(2) Å) and Pt−Br distances (2.4675(9) and 2.4687(9) Å) are comparable to those found in *cis*-coordinated bis(phosphine)platinumdibromide complexes, such as *cis*-[Ph_2-$PNHP(O)Ph_2P]_2PtBr_2$, (Pt−P (2.241(5), 2.248(4) Å); Pt−Br (2.472(2), 2.480(2) Å).[33] There is little change in the cage structure upon coordination, with P6−C5 (1.823(8), 1.845(8) Å) and P6−C7 (1.839(9), 1.852(8) Å) in **7** being somewhat shorter than the corresponding P6−C5 (1.885(2) Å; P6−C7 (1.888(2) Å) distances in **2a**.

The ^{11}B NMR spectrum of **7** showed seven overlapping resonances, and its ^{13}C NMR spectrum exhibited only one broad cage-carbon resonance. However, surprisingly, even when pure crystals of **7** were dissolved, both the ^{31}P and ^1H NMR spectra indicated the presence of another species in solution. Thus, the ^{31}P NMR spectrum showed two resonances at similar chemical shifts (−5.2 and −8.8 ppm) in an approximate 85:15 ratio intensity with both resonances exhibiting $^{31}P-^{195}Pt$ values (J_{Pt-P}, 3010 and 3010 Hz) characteristic of *cis*-coordination.[34] Likewise, the ^1H NMR spectrum showed two different bridge-hydrogen and two different CH resonances. The question then arises as to why two species are observed in solution but only one is observed in the solid state. One possible explanation is that the two rotamers shown in Figure 12, where **2a** is rotated about the Pt−P axis, exist in solution, while, in the solid state, only rotamer **A** (i.e., **7**) is present. In solution, there should be little difference in the energies of the two isomers, but, in the solid state, the structure observed for **7** could be favored owing to $\pi-\pi$ interactions of the phenyl rings. Thus, as seen in Figure

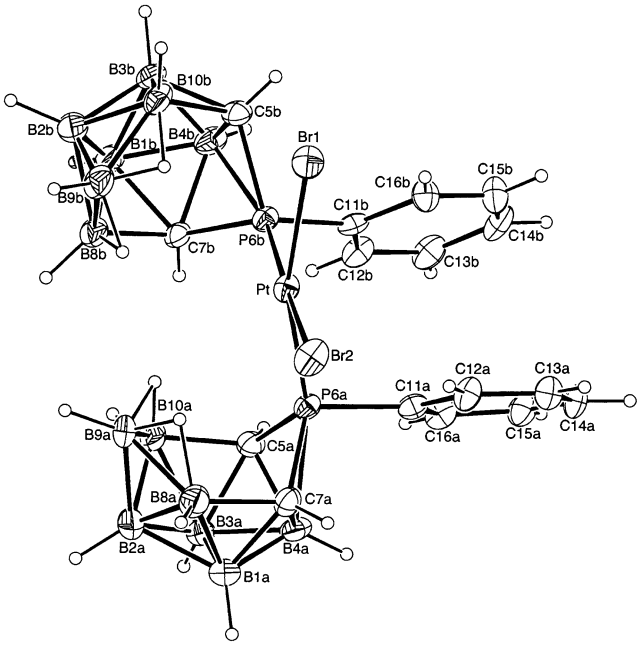

Figure 11. ORTEP drawing of *cis*-(η^1-[6-Ph-*arachno*-6,5,7-$PC_2B_7H_{11}$])$_2$-$PtBr_2$ (**7**). Selected bond distances (Å) and angles (deg): Pt−P6a, 2.254(2); Pt−P6b, 2.268(2); Pt−Br1, 2.4675(9); Pt−Br2, 2.4687(9); P6a−C11a, 1.823(9); P6a−C5a, 1.823(8); P6a−C7a, 1.839(9); P6a−B4a, 2.221(9); C5a−B10a; 1.684(13); C7a−B8a, 1.686(14); B8a−B9a, 1.814(18); B9a−B10a, 1.825(18); P6b−C11b, 1.777(9); P6b−C5b, 1.846(9); P6b−C7b, 1.852(9); P6b−B4b, 2.235(11); C5b−B10b, 1.702(15); C7b−B8b, 1.686(15); B8b−B9b, 1.814(18); B9b−B10b, 1.747(18); P6a−Pt−P6b, 95.61(7); Br1−Pt−Br2, 87.38(3); P6a−Pt−Br2, 86.91(6); P6b−Pt−Br1, 89.86(6); C11a−P6a−B4a, 90.2(4); Pt−P6a−C11a, 104.6(3); Pt−P6a−C5a, 125.0(3); Pt−P6a−C7a, 122.5(3); C11b−P6b−B4b, 88.7(4); Pt−P6b−C11b, 108.7(3); Pt−P6b−C5b, 120.9(3); Pt−P6b−C7b, 123.2(3).

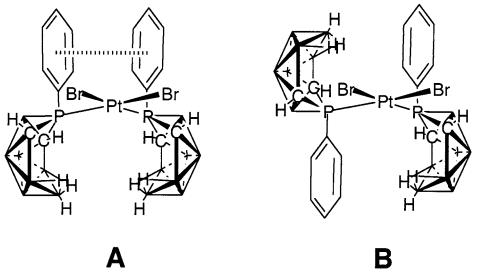

Figure 12. Possible rotomers of **7** in solution.

(30) Kang, S. O.; Sneddon, L. G. *J. Am. Chem. Soc.* **1989**, *111*, 3281−3289.
(31) Su, K.; Carroll, P. J.; Sneddon, L. G. *J. Am. Chem. Soc.* **1993**, *115*, 10004−10017.
(32) Jelínek, T.; Plesek, J.; Hermánek, S.; Stíbr, B. *Main Group Met. Chem.* **1987**, *10*, 397−398.
(33) Bhattacharyya, P.; Slawin, A. M. Z.; Smith, M. B.; Woollins, J. D. *Inorg. Chem.* **1996**, *35*, 3675−3682.
(34) Cis geometry $PtX_2(PR_3)_2$ compounds exhibit a $^1J_{Pt-P}$ of 3300−3500 Hz (e.g., *cis*-$(Me_3P)_2PtBr_2$, 3439) while trans geometries showed a $^1J_{Pt-P}$ of 2100−2600 Hz (e.g., *trans*-$(Me_3P)_2PtBr_2$, 2324). (a) Pregosin, P. S. In *Phosphorus-31 NMR Spectroscopy in Stereochemical Anaylsis*; Verkade, J. G., Quin, L. D., Eds.; VCH: New York, 1987; Chapter 14. (b) Goggin, P. L.; Goodfellow, R. J.; Haddock, S. R.; Knight, J. R.; Reed, F. J. S.; Taylor, B. F. *J. Chem. Soc., Dalton Trans.* **1974**, 523−533. (c) Favez, R.; Roulet, R.; Pinkerton, A. A.; Schwarzenbach, D. *Inorg. Chem.* **1980**, *19*, 1356−1365.

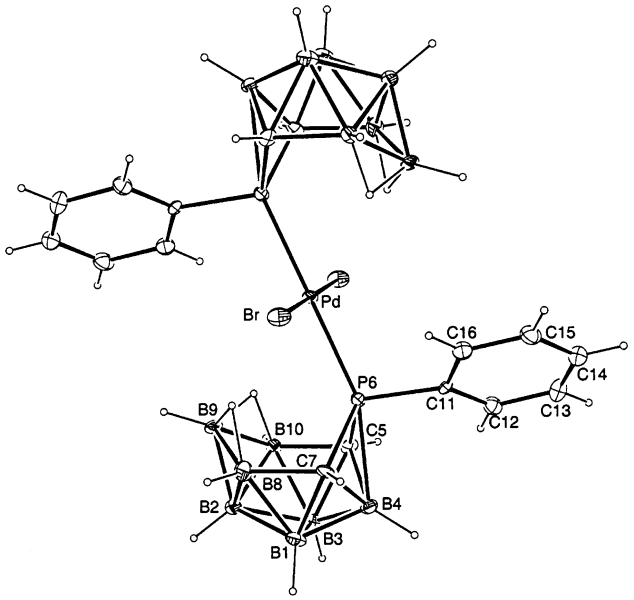

Figure 13. ORTEP drawing of *trans*-(η^1-[6-Ph-*arachno*-6,5,7-$PC_2B_7H_{11}$])$_2$-$PdBr_2$ (**8**). Selected bond distances (Å) and angles (deg): Pd−P6, 2.318(2); Pd−Br, 2.4370(7); P6−C5, 1.813(7); P6−C7, 1.843(7); C7−B8, 1.666(10); B8−B9, 1.829(12); B9−B10, 1.805(11); B10−C5, 1.678(10); P6−B4, 2.206(8); P6−Pd−Br1, 91.90(5); P6−Pd−Br2, 88.10(5); P6−Pd−P6′, 180.0; C11−P6−Pd, 105.7(2); C11−P6−C5, 109.1(3); C11−P6−C7, 111.1(3); C11−P6−B4, 93.4(3).

11, the two phenyl rings are in nearly cofacial positions with a dihedral angle of ∼7° and an interplanar distance of ∼3.5 Å. These values are quite similar to those that have been observed in other complexes with $\pi-\pi$ interactions between *cis*-coordinated aromatic ligands.[35] This $\pi-\pi$ interaction, in addition to the steric interactions of the cage, may also be a contributing factor to the larger P−Pt−P versus Br−Pt−Br bond angle.

The reaction of **2a** and $PdBr_2$ afforded a product mixture containing at least two products that were inseparable by silica gel chromatography. Although it was possible to crystallize small samples of *trans*-(η^1-[6-Ph-*arachno*-6,5,7-$PC_2B_7H_{11}$])$_2$-$PdBr_2$ (**8**) from the crude product mixture, it was not possible to isolate other products sufficiently pure to allow characterization.

$$\underset{\mathbf{2a}}{2\ \text{6-Ph-}\textit{arachno}\text{-6,5,7-}PC_2B_7H_{11}} + PdBr_2 \rightarrow \underset{\mathbf{8}}{\textit{trans}\text{-}(\eta^1\text{-[6-Ph-}\textit{arachno}\text{-6,5,7-}PC_2B_7H_{11}])_2PdBr_2} \quad (8)$$

As shown in eq 8, **8** is formed by the reaction of the palladium dibromide with 2 equiv of **2a**. A single-crystal X-ray diffraction study established the structure shown in Figure 13 in which two η^1-coordinated **2a** cages adopt a *trans*-geometry at the Pd(II) center, with P6−Pd−Br angles of 91.90(5)° and 88.10(5)° and a 180.0° P6−Pd−P6′ angle. The observed Pd−P 2.318(2) Å and Pd−Br 2.4370(7) Å distances are typical of those observed in Pd^{2+} square planar phosphine complexes, such as *trans*-[$(C_6H_4Cl)Ph_2P]_2PdBr_2$ (Pd−P, 2.350(2) and Pd−Br 2.4232(13) Å).[36] The P6−C5 (1.813(7) Å) and P6−C7 (1.843(7) Å) distances are shorter than those in **2a**, but comparable to those in the Pt complex **7**. The P6−B4 distance (2.206(8) Å) is also similar to that of **7** (2.221(9) Å).

Unlike **2a**, **1a** did not react with either $PtBr_2$ or $PdBr_2$.

Deprotonation Reactions of 1a and 2a. 2a was not deprotonated by either Proton Sponge or NaH (eq 9a). However, according to ^{11}B NMR and computational analysis, when **2a** was reacted with MeLi, a mixture of species was obtained that contained the 6-Ph-*arachno*-6,5,7-$PC_2B_7H_{10}^-$ (**2a**$^-$) anion as the predominate product. The calculated chemical shifts (−1.8 (2), −2.7 (1), −16.5 (1), −35.2 (1), and −38.7 (2) ppm) for the optimized geometry of 6-Me-*arachno*-6,5,7-$PC_2B_7H_{10}^-$ in which one of the two bridge-hydrogens of **2a** was deprotonated gave good agreement with the ^{11}B NMR chemical shifts observed for the major species present in solution.

$$\underset{\mathbf{2a}}{\text{6-Ph-}\textit{arachno}\text{-6,5,7-}PC_2B_7H_{11}} \xrightarrow[\text{or NaH}]{\text{PS}} \text{No reaction} \quad (9a)$$

$$\underset{\mathbf{2a}}{\text{6-Ph-}\textit{arachno}\text{-6,5,7-}PC_2B_7H_{11}} \xrightarrow{\text{MeLi}} \underset{\mathbf{2a^-}}{\text{6-Ph-}\textit{arachno}\text{-6,5,7-}PC_2B_7H_{10}^-} \quad (9b)$$

On the other hand, the 6-Ph-*arachno*-6,8,9-$PC_2B_7H_{10}^-$ (**1a**$^-$) monoanion was cleanly obtained by the reaction of **1a** with Proton Sponge or NaH (eq 10).

$$\underset{\mathbf{1a}}{\text{6-Ph-}\textit{arachno}\text{-6,8,9-}PC_2B_7H_{11}} \xrightarrow{\text{PS or NaH}} \underset{\mathbf{1a^-}}{\text{6-Ph-}\textit{arachno}\text{-6,8,9-}PC_2B_7H_{10}^-} \quad (10)$$

Since **1a** has two potentially acidic hydrogens, a bridge-hydrogen spanning B5−B10 and an *endo*-hydrogen at C9, mono-deprotonation could in principle yield analogues of either of the structures, **Ib$_1$**$^-$ or **Ib$_2$**$^-$, shown in Figure 14a and 14b. DFT calculations showed that structure **Ib$_1$**$^-$, in which the bridge-hydrogen at B5−B10 was removed, is 7.6 kcal/mol more favored than the *endo*-C9 deprotonated structure **Ib$_2$**$^-$, and indeed, the DFT/GIAO calculated chemical shifts for **Ib$_1$**$^-$ showed better agreement with the experimental data for **1a**$^-$ than those calculated for structure **Ib$_2$**$^-$ (Table 1). A comparison of the calculated bond distances and angles for **Ib$_1$**$^-$ with those found for the neutral compound **Ib** reveals that the major structural change that occurs upon deprotonation of the B5−B10 bridge-hydrogen is a significant shortening of B5−B10 to 1.720 Å and an elongation of B2−C9 to 1.806 Å compared to their values in **Ib** (B5−B10, 1.872 Å; B2−C9, 1.738 Å).

The 6-Ph-*arachno*-6,8,9-$PC_2B_7H_9^{2-}$ (**1a**$^{2-}$) dianion was prepared by reaction with the stronger base MeLi in DME solution (eq 11).

$$\underset{\mathbf{1a}}{\text{6-Ph-}\textit{arachno}\text{-6,8,9-}PC_2B_7H_{11}} \xrightarrow{\text{2 equiv of MeLi}} \underset{\mathbf{1a^{2-}}}{\text{6-Ph-}\textit{arachno}\text{-6,8,9-}PC_2B_7H_9^{2-}} \quad (11)$$

The DFT/GIAO calculated chemical shifts for structure **Ib**$^{2-}$ shown in Figure 14c, in which both the B5−B10 and *endo*-C9 hydrogens have been removed, showed good agreement with

(35) (a) Hirsivaara, L.; Haukka, M.; Pursiainen, J. *Eur. J. Inorg. Chem.* **2001**, *9*, 2255−2262. (b) Yang, F.; Fanwick, P. E.; Kubiak, C. P. *Inorg. Chem.* **2002**, *41*, 4805−4809.
(36) Coalter, N. L.; Concolino, T. E.; Streib, W. E.; Hughes, C. G.; Rheingold, A. L.; Zaleski, J. M. *J. Am. Chem. Soc.* **2000**, *122*, 3112−3117.

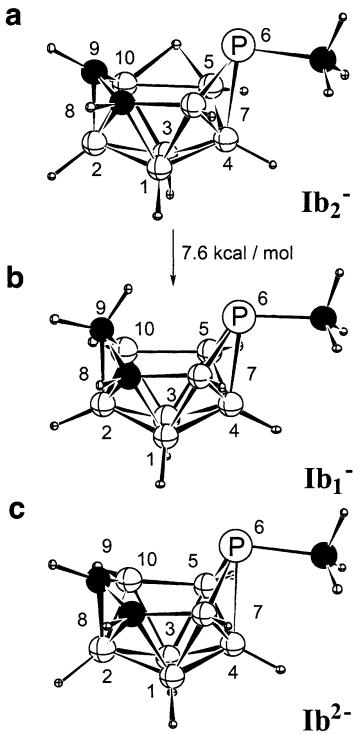

Figure 14. DFT optimized geometries (B3LYP/6-311G*//B3LYP/6-311G*) of two possible monoanions of 6-R-*arachno*-6,8,9-$PC_2B_7H_{10}^-$ (**Ib$_1^-$**, **Ib$_2^-$**) and a dianion 6-R-*arachno*-6,8,9-$PC_2B_7H_{10}^{2-}$ (**Ib^{2-}**). Selected bond distances (Å) and angles (deg) for **Ib$_1^-$** and **Ib^{2-}**. **Ib$_1^-$**: B5−P6, 1.998; P6−B7, 1.984; B7−C8, 1.606; C8−C9, 1.570; C9−B10, 1.733; B10−B5, 1.720; P6−B4, 2.092; B2−C9, 1.806; P6−C11, 1.888; B4−P6−C11, 93.2; C8−C9−B10, 107.5, B5−P6−B7, 94.3. **I^{2-}**: B5−P6, 2.005; P6−B7, 2.001; B7−C8, 1.605; C8−C9, 1.498; C9−B10, 1.575; B10−B5, 1.742; P6−B4, 2.297; B2−C9, 1.608; P6−C11, 1.931; B4−P6−C11, 86.8; C8−C9−B10, 114.8; B5−P6−B7, 89.0.

the ^{11}B NMR spectrum of **1a^{2-}** (Table 1). An examination of the dianion structure reveals several significant cage structural changes compared to either **Ib** or **Ib$_1^-$**. Most notably, in the dianion, the deprotonation of the *endo*-C9−H has greatly increased the bonding interactions of the C9 carbon with its neighboring cage atoms, with the C8−C9 (1.498 Å), C9−B10 (1.575 Å), and C9−B2 (1.608 Å) distances all being dramatically shortened compared to their values in either **Ib** (1.577, 1.774, and 1.738 Å, respectively) or **Ib$_1^-$** (1.570, 1.733, and 1.806 Å, respectively).

Coordination Chemistry of the 6-Ph-*arachno*-6,8,9-$PC_2B_7H_9^{2-}$ (1a^{2-}) Anion. The reaction of the 6-Ph-*arachno*-6,8,9-$PC_2B_7H_9^{2-}$ (**1a^{2-}**) anion with $(Ph_3P)_2PtCl_2$ gave 8-Ph-7-$(Ph_3P)_2$-*nido*-7,8,10,11-$PtPC_2B_7H_9$ (**9**, eq 12).

$$\underset{\mathbf{1a^{2-}}}{Li_2^+[\text{6-Ph-}\textit{arachno}\text{-6,8,9-}PC_2B_7H_9^{2-}]} + (Ph_3P)_2PtCl_2 \rightarrow \underset{\mathbf{9}}{\text{8-Ph-7-}(Ph_3P)_2\text{-}\textit{nido}\text{-7,8,10,11-}PtPC_2B_7H_9} + 2\ LiCl \quad (12)$$

Likewise, the reaction (eq 13) of 6-Ph-*arachno*-6,8,9-$PC_2B_7H_{11}$ (**1a**) with $CpCo(CO)_2$ at 70 °C resulted in the oxidative insertion[37] of the cobalt into the cage to produce the 7-Ph-11-(η^5-C_5H_5)-*nido*-11,7,9,10-$CoPC_2B_7H_9$ (**10**) complex in which a Co^{3+} ion is sandwiched between formal η^5-$C_5H_5^-$ and η^4-6,8,9-$PC_2B_7H_9^{2-}$ (**1a^{2-}**) anions.

$$\underset{\mathbf{1a}}{\text{6-Ph-}\textit{arachno}\text{-6,8,9-}PC_2B_7H_{11}} + CpCo(CO)_2 \xrightarrow{-2\ CO,\ H_2} \underset{\mathbf{10}}{\text{7-Ph-11-Cp-}\textit{nido}\text{-11,7,9,10-}CoPC_2B_7H_9} \quad (13)$$

In agreement with their predicted 26 skeletal electron counts,[19] single-crystal X-ray diffraction studies of **9** and **10** established the 11-vertex *nido*-cluster structures shown in Figures 15 and 16. The phosphadicarbaboranyl ligands are each coordinated to the metals in an η^4-fashion. In both complexes, the heteroatoms occupy low connectivity sites on the five-membered open face of the cluster with the Pt in **9** and the Co in **10** being slightly distorted above the plane of the other four facial atoms. Similar η^4-coordination was observed for the isoelectronic phosphamonocarbaborane 6-Ph-*arachno*-$PCB_8H_{10}^{2-}$ anion in the Pt^{2+} complex 7-Ph-11-$(Ph_3P)_2$-*nido*-11,7,8-$PtPCB_8H_{10}$,[2b] and in both this complex and **9**, the dihedral angle between the five-membered open face and the P18−Pt11−P37 plane is ∼73°. In contrast to **7** where the P6a−Pt−P6b angle is 95.61(7)°, in **9** the P18−Pt−P37 angle has increased to 101.46(5)° consistent with the expected change in platinum hybridization upon insertion. The Pt−P bond length in **9** (2.4208(14)Å) is also longer than those observed in **7** (2.254(2) and 2.268(2)Å).

Consistent with the crystallographically established structures, the ^{11}B NMR spectra of **9** and **10** each showed seven resonances, their ^{13}C NMR spectrum each exhibited two cage-carbon resonances, and their ^{1}H NMR spectra showed the appropriate BH and CH resonances. The ^{31}P NMR spectrum of **9** showed three resonances, each of which were coupled to ^{195}Pt (J_{Pt-P}, 3596, 4218, 4236 Hz). The phosphorus resonances of the two Ph_3P groups showed additional doublet structure (J_{PP}, 17, 18 Hz) arising from coupling to the cage phosphorus, and accordingly, although not clearly resolved, the cage phosphorus resonance showed the corresponding triplet fine-structure from coupling to the two Ph_3P phosphorus atoms.

The reaction (eq 14) of 2 equiv of the 6-Ph-*arachno*-6,8,9-$PC_2B_7H_{10}^-$ (**1a$^-$**) anion with $NiBr_2$ followed by an oxidative workup produced *commo*-Ni-(7-Ni-8′-Ph-*nido*-8′,10′,11′-$PC_2B_7H_9$)(7-Ni-8-Ph-*nido*-8,10,11-$PC_2B_7H_9$) (**11**).

$$2\ \underset{\mathbf{1a^-}}{Li^+[\text{6-Ph-}\textit{arachno}\text{-6,8,9-}PC_2B_7H_{10}^-]} + NiBr_2 \xrightarrow[(2)\ O_2,\ -H_2O]{(1)\ -2\ LiBr} \underset{\mathbf{11}}{\textit{commo}\text{-Ni-(7-Ni-8′-Ph-}\textit{nido}\text{-8′,10′,11′-}PC_2B_7H_9)\text{-}(\text{7-Ni-8-Ph-}\textit{nido}\text{-8,10,11-}PC_2B_7H_9)} \quad (14)$$

Owing to the C_1 symmetries of the 6-Ph-*arachno*-6,8,9-$PC_2B_7H_{10}^-$ (**1a$^-$**) and 6-Ph-*arachno*-6,8,9-$PC_2B_7H_9^{2-}$ (**1a^{2-}**) anions, they are each synthesized as racemic mixtures. Thus, when a bis-cage complex, such as **11**, is formed from one of these anions, it could result from reaction with 2 equiv of the same enantiomer (*R*−M−*R* or *S*−M−*S* complexes) or from reaction with the two different enantiomeric forms of the anion (*R*−M−*S*).[38] The single-crystal X-ray diffraction study of **11** (Figure 17) established that two phosphadicarbaboranyl ligands

(37) (a) Miller, V. R.; Sneddon, L. G.; Beer, D. C.; Grimes, R. N. *J. Am. Chem. Soc.* **1974**, *96*, 3090−3098. (b) Maxwell, W. M.; Grimes, R. N. *Inorg. Chem.* **1979**, *18*, 2174−2178. (c) Grimes, R. N. In *Comprehensive Organometallic Chemistry*; Wilkinson, G., Ed.; Pergamon: New York, 1982; Vol. 1, Chapter 5.5.

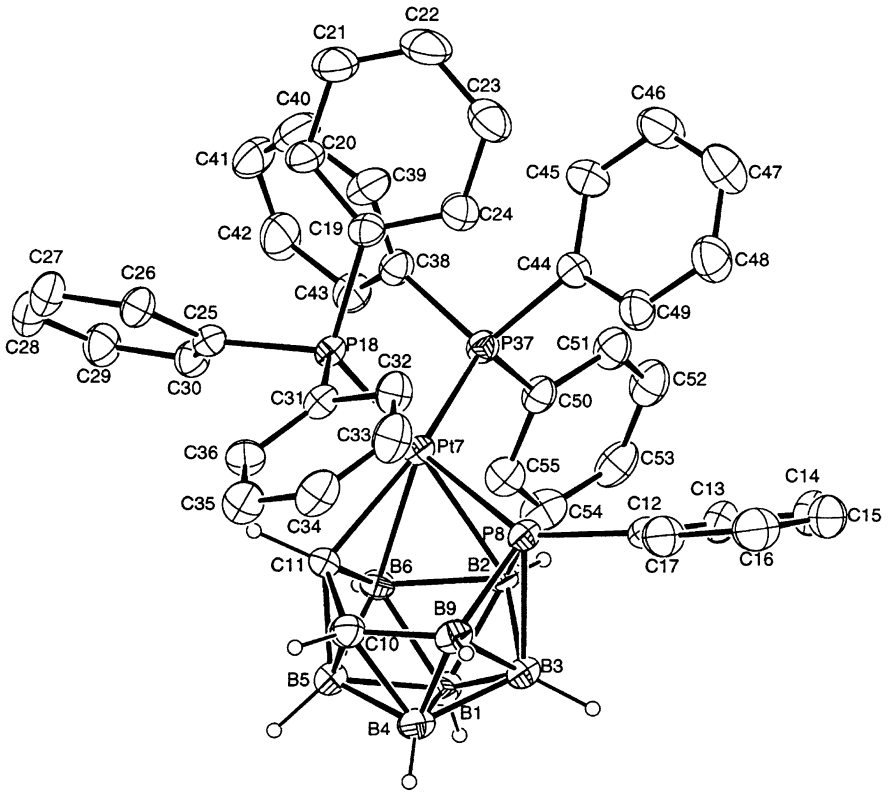

Figure 15. ORTEP drawing of 8-Ph-7-$(Ph_3P)_2$-*nido*-7,8,10,11-$PtPC_2B_7H_9$ (**9**). Selected bond distances (Å) and angles (deg): Pt7−P8, 2.4208(14); Pt7−B2, 2.273(6); Pt7−B6, 2.210(5); Pt7−C11, 2.176(5); P8−B9, 1.928(7); B9−C10, 1.639(11); C10−C11, 1.522(8); Pt7−P37, 2.3164(15); Pt7−P18, 2.3061(16); P8−Pt7−P18, 108.61(5); P8−Pt7−P37, 118.25(5); P18−Pt7−P37, 101.46(5); C11−Pt7−P37, 151.68(15); C11−Pt7−P18, 88.46(17).

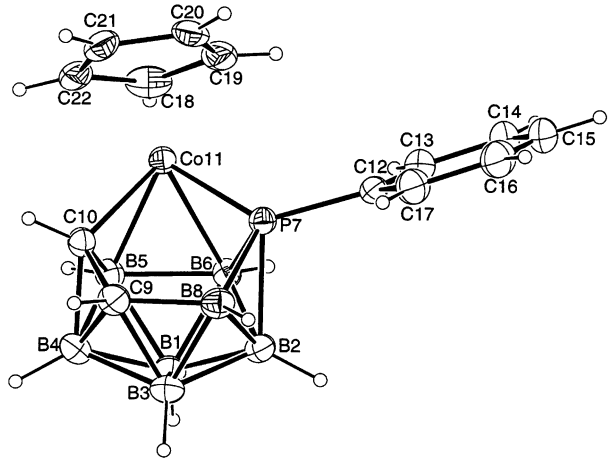

Figure 16. ORTEP drawing of 7-Ph-11-(η^5-C_5H_5)-*nido*-11,7,9,10-$CoPC_2B_7H_9$ (**10**). Selected bond distances (Å) and angles (deg): P7−B8, 1.899(3); B8−C9, 1.632(4); C9−C10, 1.527(3); Co11−P7, 2.1378(7); Co11−C10, 2.003(2); Co11−B5, 2.059(3); Co11−B6, 2.140(3); P7−C12, 1.802(2); C12−P7−B2, 107.05(12); C12−P7−Co11, 127.86(8); Co11−P7−B8, 111.22(11); P7−B8−C9, 103.34(19); B8−C9−C10, 117.9(2); C9−C10−Co11, 120.67(17); C10−Co11−P7, 86.26(8).

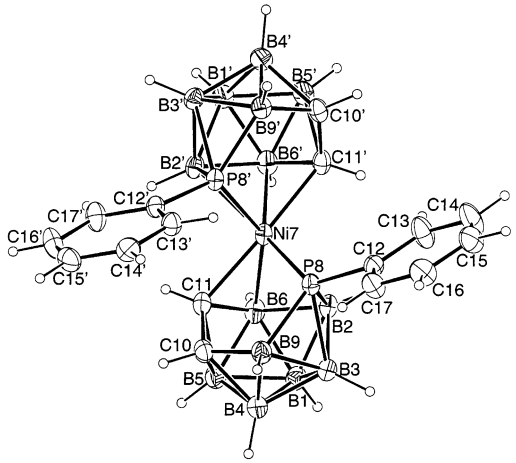

Figure 17. ORTEP drawing of *commo*-Ni-(7-Ni-8′-Ph-*nido*-8′,10′,11′-$PC_2B_7H_9$)(7-Ni-8-Ph-*nido*-8,10,11-$PC_2B_7H_9$) (**11**). Selected bond distances (Å) and angles (deg): Ni7−P8, 2.1837(6); Ni7−C11, 2.055(2); Ni7−B2, 2.165(3); Ni7−B6; 2.117(3); P8−B9, 1.895(3); B9−C10, 1.652(4); C10−C11, 1.501(3); P8−B2, 2.008(3); P8−C12, 1.792(3); Ni7−P8′, 2.1692(6); Ni7−C11′, 2.061(2); Ni7−B2′, 2.169(3); Ni7−B6′, 2.120(3); P8′−B9′, 1.899(3); B9′−C10′, 1.654(4); C10′−C11′, 1.518(3); P8′−B2′, 1.995(3); P8−Ni7−P8′, 92.13(2); P8−Ni7−C11′, 102.45(7); P8′−Ni7−C11, 97.73(7); C11−Ni7−P8, 88.35(7); Ni7−P8−B9, 107.41(10); P8−B9−C10, 106.2(2); B9−C10−C11, 119.0(2); C10−C11−Ni7, 117.54(17); C11′−Ni7−P8′, 89.16(7); Ni7−P8′−B9′, 107.53(9); P8′−B9′−C10′, 106.03(18); B9′−C10′−C11′, 119.5(2); C10′−C11′−Ni7, 116.16(16); Ni7−P8′−C12′, 124.94(8).

of the same enantiomeric type (both *R*-M-*R* and *S*-M-*S* complexes being present in the $P2_1/c$ unit cell) are η^4-coordinated to the nickel center. The nickel center occupies a four-coordinate vertex in each cage, with both cages adopting 11-vertex *nido*-structures similar to those found for **9** and **10**.

In both cages, all of the heteroatoms are present on the open pentagonal face and the two cages are twisted 64.9(1)° (as measured by the dihedral angle between the B1′−B4′−Ni7 and B1−B4−Ni7 planes) with a 84.00(5)° angle between the planes of the two open pentagonal faces. Since **11** has two anions of

(38) A modification of the *R* and *S* notation for configuration specification is utilized here. Observation of the phosphadicarbaborane cage from the open face is thus prioritized from the phosphorus, where the configuration is specified *R*, for a clockwise direction, or *S*, for the counterclockwise configuration.

the same enantiomeric type, these cages are related by a noncrystallographic C_2 axis passing through the nickel ion, and all of the NMR spectral data for **11** likewise indicate that the two cages are equivalent. TLC, mass spectroscopy, and NMR analysis of the reaction mixture also indicated the production of another isomeric complex. This complex could not be isolated in sufficient purity to allow complete characterization; however, its more complex NMR spectra suggest that it is most likely the *R*−M−*S* complex.

Since complex **11** contains two 6-Ph-*arachno*-6,8,9-$PC_2B_7H_9^{2-}$ (**1a**$^{2-}$) dianion ligands, the nickel has a formal oxidation state of Ni^{4+}. Thus the **1a**$^{2-}$ dianion appears to have an ability, similar to that of the dicarbabollide $C_2B_9H_{11}^{2-}$ dianions in *closo*-Ni-$(C_2B_9H_{11})_2$,[39] to stabilize high oxidation states. The Ni−C11 and Ni−C11′ (2.055(2) and 2.061(2) Å) and the Ni7−B2, Ni7−B2′, Ni7−B6, and Ni7−B6′ distances (2.165(3), 2.169(3), 2.117(3), and 2.120(3) Å) in **11** are reasonably similar to the Ni−C (2.077(2), 2.065(2), 2.072(2), and 2.071(2) Å) and Ni−B distances (2.105(2), 2.086(2), and 2.120(2) Å) in *closo*-Ni-$(C_2B_9H_{11})_2$.[40]

In conclusion, these studies have resulted in the syntheses and structural characterizations of two isomers of the first 10-vertex phosphadicarbaboranes. While DFT calculations showed that the HOMO orbitals of both isomers have large components at their *endo*-P6 positions, the isomers exhibit very different chemistries, with only the 6-R-*arachno*-6,5,7-$PC_2B_7H_{11}$ (**2**) isomer showing strong donor properties, forming *endo*-L-*exo*-6-R-*arachno*-6,5,7-$PC_2B_7H_{11}$ (L = BH_3 (**3**), S (**4**), O (**5**), Pt (**7**), and Pd (**8**)) complexes containing Lewis acidic substituents bonded at the *endo*-position of the P6-phosphorus. These donor properties are similar to those recently reported for the isoelectronic 6-R-*arachno*-6,7-$PCB_8H_{11}^-$ phosphamonocarbaborane anion.[2] Thus 6-R-*arachno*-6,7-$PCB_8H_{11}^-$ and **2** can be considered anionic and neutral phosphacarbaborane analogues, respectively, of an R_3P donor. The differences in Lewis basicities found for **2** and 6-R-*arachno*-6,8,9-$PC_2B_7H_{11}$ (**1**) is most likely a consequence of the fact that the phosphorus in **1** is directly bonded to three electron-poor borons and can readily delocalize electron density to these atoms, whereas in **2** the phosphorus is adjacent to two electron-donating carbons that enhance the phosphorus donor properties. While neutral **1** does not coordinate with transition metals, its dianion readily coordinates to transition metals in an η^4-fashion and appears to have an ability, like the dicarbollide dianion, to stabilize metals in high oxidation states.

Acknowledgment. We thank the National Science Foundation for the support of this research.

Supporting Information Available: Tables listing Cartesian coordinates for DFT optimized geometries. X-ray crystallographic data for structure determinations of compounds **1a**, **2a**, **7**, **8**, **9**, **10**, and **11** (CIF). This material is available free of charge via the Internet at http://pubs.acs.org.

JA037799+

(39) Warren, L. F., Jr.; Hawthorne, M. F. *J. Am. Chem. Soc.* **1970**, *92*, 1157−1173.
(40) St. Clair, D.; Zalkin, A.; Templeton, D. H. *J. Am. Chem. Soc.* **1970**, *92*, 1173−1179.